

# Quaternary Science Reviews

## Late Quaternary palaeoenvironmental evolution of the south-eastern Alpine foreland basin from multi-proxy analysis

--Manuscript Draft--

<b>Manuscript Number:</b>	
<b>Article Type:</b>	Research Paper
<b>Keywords:</b>	Middle and Upper Pleistocene glaciations; Venetian plain; Chrono- biostratigraphy; Vegetation dynamics; Sedimentary evolution; Alluvial successions
<b>Corresponding Author:</b>	Arianna Marcolla Universita degli Studi di Padova ITALY
<b>First Author:</b>	Arianna Marcolla
<b>Order of Authors:</b>	Arianna Marcolla Antonella Miola Paolo Mozzi Giovanni Monegato Alessandra Asioli Roberta Pini Cristina Stefani
<b>Abstract:</b>	<p>The multidisciplinary analysis of two long sedimentary successions of continental and shallow marine deposits from the Venetian plain (NE Italy), provides new data on the stratigraphic architecture and the landscape evolution of the south-eastern Alpine foreland basin during the last 210-220 ka, with further evidences of a warm temperate phase older than MIS 8. We present and discuss a detailed multi-proxy data set from these successions (GER1 and CB cores). The results of stratigraphic, palynological and micropaleontological analyses are cross-interpreted, showing the potentiality of building a composite section of two close continental successions within the same alluvial system, the Brenta megafan, with 15 km distance between cores along a downstream direction. The chronology of the upper part of the cores is supported by radiocarbon dating, showing the presence of Last Glacial Maximum (LGM) and post-LGM fluvial deposits. Lower down, the estimated chronology relies on the tight integration between palynostratigraphy and lithostratigraphy, as well as on the correlation with other regional biostratigraphic records and the Northern Hemisphere/global isotopic record. The only marine transgression present in the studied successions is attributed to the MIS 7c and constitutes the basal tiepoint for the correlation between the two cores. Below the MIS 7c transgressive marine surface is a fluvial succession with weakly-developed paleosoils and scant pollen content suggesting cold climate (possibly MIS 8), that lies on top of a thick peat showing palynological evidence of a warm temperate climate. The occurrence of well-preserved <i>Pterocarya</i> pollen in the basal peat level (GER1 core) provides new insights for the chronological framing of the problematic last occurrence of <i>Pterocarya</i> in the southern alpine area. Whilst mixed temperate forest persisted throughout MIS 7c-7a, conifers spread during MIS 6. By this time, a glaciofluvial aggradation phase is recorded, highlighting the strong relationship between glacial maxima and alluvial aggradation in the Venetian plain. None of the drilling sites were reached by the Last Interglacial sea transgression. However, the Eemian forest signature is well recorded in CB core, and the following Early to Middle Würm stadial-interstadial sequence is clearly outlined thanks to the joint analysis of the two successions. Broad-leaved thermophilous forests disappeared at the end of the Early Würm and only <i>Pinus</i> and <i>Betula</i> persisted throughout the LGM, during which a chronologically well-constrained glaciofluvial aggradation occurred. The last depositional event corresponds to the post-LGM cut-and-fill of fluvial incised valleys in GER1 core, and to soil evolution and very thin burial by Brenta River fluvial deposits in CB core.</p>

<b>Suggested Reviewers:</b>	Donatella Magri donatella.magri@uniroma1.it
	Pedro Manuel Rodrigues Roque Proença e Cunha pcunha@dct.uc.pt
	Pierluigi Pieruccini pierluigi.pieruccini@unito.it
	Jürgen Reitner juergen.reitner@geologie.ac.at

To Editorial Office  
Quaternary Science Reviews

**Dear Editors,**

I submit to Quaternary Science Reviews a manuscript about the climatic and stratigraphic evolution of the Venetian Plain (NE Italy) during the late Quaternary:

**Late Quaternary palaeoenvironmental evolution of the south-eastern Alpine foreland basin  
from multi-proxy analysis**

A. Marcolla\*, A. Miola, P. Mozzi, G. Monegato, A. Asioli, R. Pini, C. Stefani

\* Corresponding author: [arianna.marcolla@phd.unipd.it](mailto:arianna.marcolla@phd.unipd.it)

The research gives an important contribution to the knowledge about the stratigraphic, climatic and environmental evolution of the Venetian plain (NE Italy) since the Middle Pleistocene and enriches the proxy dataset available in the south-eastern Alpine foreland basin.

With the present letter I am stating that:

- All authors contributed substantially to the research. Arianna Marcolla: Investigation, Data analysis, Writing – Original draft preparation; Antonella Miola: Investigation, Methodology, Data analysis; Paolo Mozzi: Conceptualization, Investigation, Writing – Review & Editing; Giovanni Monegato: Conceptualization, Validation, Writing – Review & Editing; Alessandra Asioli: Investigation, Data analysis; Roberta Pini: Validation, Writing – Review & Editing; Cristina Stefani: Conceptualization, Supervision;
- The final version of the manuscript is approved by all the authors;
- The manuscript is original and it has not been submitted for publication until now, or until your revision has been finished;
- The included figures are original;
- The authors have no known competing financial interests or personal relationships that could have appeared to influence the work reported in this paper.

Possible reviewers for this subject are:

- Prof. Donatella Magri - [donatella.magri@uniroma1.it](mailto:donatella.magri@uniroma1.it)
- Prof. Pedro Manuel Rodrigues Roque Proença e Cunha - [pcunha@dct.uc.pt](mailto:pcunha@dct.uc.pt)
- Prof. Pierluigi Pieruccini - [pierluigi.pieruccini@unito.it](mailto:pierluigi.pieruccini@unito.it)
- Dr. Jürgen M. Reitner - [juergen.reitner@geologie.ac.at](mailto:juergen.reitner@geologie.ac.at)

July 03, 2020

*Arianna Marcolla.....*

## Highlights

- The last two glacial cycles are well recorded in Central Venetian plain (NE Italy).
- Thick alluvial aggradation phases correlate to glacial culminations in the Alps.
- MIS 7.3 transgression is recorded as proximal marine facies in C. Venetian plain.
- Continental conditions persisted in C. Venetian plain during MIS 5.5 sea highstand.
- *Pterocarya* is only present in sediments older than 220 ka.

1 **Late Quaternary palaeoenvironmental evolution of the south-eastern Alpine foreland basin**  
2 **from multi-proxy analysis**

3  
4 A. Marcolla<sup>a,\*</sup>, A. Miola<sup>b</sup>, P. Mozzi<sup>a</sup>, G. Monegato<sup>c</sup>, A. Asioli<sup>d</sup>, R. Pini<sup>e</sup>, C. Stefani<sup>a</sup>

5  
6 <sup>a</sup> Department of Geosciences, University of Padova, Via Gradenigo 6, 35131, Padova, Italy;

7 <sup>b</sup> Department of Biology, University of Padova, Via Ugo Bassi 58/B, 35131 Padova, Italy;

8 <sup>c</sup> CNR-IGG, Via Gradenigo 6, 35131, Padova, Italy;

9 <sup>d</sup> CNR-ISMAR, Via Piero Gobetti 101, 40129, Bologna, Italy;

10 <sup>e</sup> CNR-IGAG, Lab. of Palynology and Palaeoecology, Piazza della Scienza 1, 20126 Milano, Italy

11

12 \* Corresponding author: [arianna.marcolla@phd.unipd.it](mailto:arianna.marcolla@phd.unipd.it)

13

14 **Abstract**

15 The multidisciplinary analysis of two long sedimentary successions of continental and shallow marine  
16 deposits from the Venetian plain (NE Italy), provides new data on the stratigraphic architecture and  
17 the landscape evolution of the south-eastern Alpine foreland basin during the last 210-220 ka, with  
18 further evidences of a warm temperate phase older than MIS 8.

19 We present and discuss a detailed multi-proxy data set from these successions (GER1 and CB cores).  
20 The results of stratigraphic, palynological and micropaleontological analyses are cross-interpreted,  
21 showing the potentiality of building a composite section of two close continental successions within  
22 the same alluvial system, the Brenta megafan, with 15 km distance between cores along a downstream  
23 direction. The chronology of the upper part of the cores is supported by radiocarbon dating, showing  
24 the presence of Last Glacial Maximum (LGM) and post-LGM fluvial deposits. Lower down, the  
25 estimated chronology relies on the tight integration between palynostratigraphy and lithostratigraphy,

26 as well as on the correlation with other regional biostratigraphic records and the Northern  
27 Hemisphere/global isotopic record.

28 The only marine transgression present in the studied successions is attributed to the MIS 7c and  
29 constitutes the basal tiepoint for the correlation between the two cores. Below the MIS 7c  
30 transgressive marine surface is a fluvial succession with weakly-developed paleosoils and scant  
31 pollen content suggesting cold climate (possibly MIS 8), that lies on top of a thick peat showing  
32 palynological evidence of a warm temperate climate. The occurrence of well-preserved *Pterocarya*  
33 pollen in the basal peat level (GER1 core) provides new insights for the chronological framing of the  
34 problematic last occurrence of *Pterocarya* in the southern alpine area.

35 Whilst mixed temperate forest persisted throughout MIS 7c-7a, conifers spread during MIS 6. By this  
36 time, a glaciofluvial aggradation phase is recorded, highlighting the strong relationship between  
37 glacial maxima and alluvial aggradation in the Venetian plain. None of the drilling sites were reached  
38 by the Last Interglacial sea transgression. However, the Eemian forest signature is well recorded in  
39 CB core, and the following Early to Middle Würm stadial-interstadial sequence is clearly outlined  
40 thanks to the joint analysis of the two successions. Broad-leaved thermophilous forests disappeared  
41 at the end of the Early Würm and only *Pinus* and *Betula* persisted throughout the LGM, during which  
42 a chronologically well-constrained glaciofluvial aggradation occurred. The last depositional event  
43 corresponds to the post-LGM cut-and-fill of fluvial incised valleys in GER1 core, and to soil  
44 evolution and very thin burial by Brenta River fluvial deposits in CB core.

45 **Keywords:** Middle and Upper Pleistocene glaciations; Venetian plain; Chrono- biostratigraphy;

46 Vegetation dynamics; Sedimentary evolution; Alluvial successions

47

## 48 **1. Introduction**

49 The European Alps and their forelands are key areas for detecting Quaternary climate and  
50 environmental variations, as they provide different valuable proxies for regional reconstructions of  
51 vegetation (e.g., Grüger, 1989; Drescher-Schneider, 2000; Müller et al., 2003; Pini et al., 2009, 2010;

52 Monegato et al., 2010, 2015; Duprat-Oualid et al., 2017), climate (e.g., Spötl et al., 2007; Heiri et al.,  
53 2014; Luetscher et al., 2015) and sedimentary systems (e.g., Garzanti et al., 2011; Fontana et al.,  
54 2014). Improving of these datasets in terms of accuracy, time resolution and time scales is crucial for  
55 the development of robust paleoclimate reconstructions that can allow better understanding of global  
56 circulation during climatic extremes (Martinson et al., 1987; Siddall et al., 2006; Braconnot et al.,  
57 2007; Löffverström et al., 2014; Löffverström, 2020).

58 The south-eastern Alpine foreland basin lies between the Mediterranean region and the southern side  
59 of the Alps (Fig. 1). It shows considerable subsidence rates (0.5 - 1.3 mm/yr; Bortolami et al., 1984;  
60 Carbognin et al., 2002, Kent et al., 2002) that causes the Venetian-Friulian plain to act as a  
61 sedimentary basin, preserving stratigraphic evidence of local climatic fluctuations, as well as of the  
62 Middle-Late Pleistocene global glacioeustatic cycles (Kent et al., 2002; Massari et al., 2004; Pini et  
63 al., 2009; Monegato et al., 2011). Its sedimentary evolution since the onset of the Pleistocene  
64 glaciations (Muttoni et al., 2003) has been strongly influenced by glacial-interglacial cycles. These  
65 caused the development of glacier piedmont lobes during cold periods (Monegato et al., 2007; 2017),  
66 even in relatively small alpine catchments, while the proximity of the Adriatic Sea led to marine  
67 transgressions during interglacial periods.

68 The thick glaciofluvial succession related to the aggradation phase of the Last Glacial Maximum  
69 (LGM, 26.5-19 ka, Clark et al., 2009) provided valuable evidence for detailed reconstructions of the  
70 climatic and environmental changes occurred since the LGM (Mozzi, 2005; Miola et al., 2006; Mozzi  
71 et al., 2010; Monegato et al., 2011; Fontana et al., 2008, 2010a, 2014; Rossato et al., 2018).  
72 Conversely, information on the pre-LGM evolution are scarce because of the significant depth,  
73 generally more than 30 meters, at which the relative sediments are found (Fontana et al., 2010a),  
74 while the cropping out of the succession is scattered and limited (Venzo, 1977; Monegato et al., 2010;  
75 Rossato et al., 2013).

76 The available continuous stratigraphic records, whose investigation provided information on the last  
77 climatic cycles older than the LGM in the Venetian-Friulian plain, are Venezia1 core (Müllenders et

78 al., 1996; Massari et al., 2004), the AzzanoX core (Zanferrari et al., 2008; Pini et al., 2009), and Lake  
79 Fimon cores (Pini et al., 2010; Monegato et al., 2011, Fig. 1). These last two provided continuous and  
80 detailed biostratigraphic records for the last glacial-interglacial cycles and are, therefore, reference  
81 cores for the correlation of pre-LGM successions in the Venetian-Friulian plain.

82 In the present work, we reconstruct the palaeoenvironmental and vegetation history in the central  
83 Venetian plain since the Middle Pleistocene, basing on the palynology, micropaleontology, physical  
84 stratigraphy and radiocarbon dating of two long cores: the new Geriatrico 1 core (GER1), 130 m deep,  
85 and the Ca' Borille core (CB), 103 m deep, only partly studied by Cucato et al. (2012). We  
86 furthermore discuss regional stratigraphic correlations with other master cores in the Venetian-  
87 Friulian plain and surrounding areas. The main aim of this research is to reconstruct the sedimentary  
88 and environmental evolution of this foreland basin in relation to global climatic and eustatic changes.  
89 The studied boreholes lie close to both the mouth of major Alpine valleys (i.e. Brenta, Astico and  
90 Piave valleys) and the Venice Lagoon and Adriatic coastal plain. Their centrality between the Alps  
91 and the Adriatic Sea makes them key sites for analyzing the relative forcing of mountain glaciations  
92 and glacio-eustatic fluctuations on the alluvial and coastal systems.

93

## 94 **2. Geological setting**

95 The Venetian-Friulian plain is part of the foreland basin of the Southern Alps (e.g., Massari et al.,  
96 1986; Stefani et al., 2007; Mancin et al., 2009) and, though geographically-speaking it is the eastern  
97 extension of the so-called Po Plain, it has been formed by rivers that are not presently tributaries of  
98 the Po River (Castiglioni, 1999).

99 Since the Mesozoic, its structural setting was affected by the combined dynamics of the Southern  
100 Alps, the Northern Apennines and the External Dinarides, which led to a complex and fragmented  
101 architecture, influencing the deposition of the sediments during the Quaternary (e.g., Massari et al.,  
102 1986; Pola et al., 2014; Toscani et al., 2016). This configuration has led to a persistent subsidence,  
103 affecting the area during the Middle-Late Pleistocene and still ongoing (Carbognin et al., 2002; Kent



104 et al., 2002), which determined the sensitivity of the plain to the major eustatic fluctuations, with the  
105 consequent alternate deposition of continental, transitional and marine sedimentary units. The study  
106 area is located close to the SW boundary of the Venetian-Friulian foredeep, that is marked by the  
107 NW-SE trending, active Schio-Vicenza strike-slip fault system (Pola et al., 2014 and references  
108 therein).

109 Large sectors of the present surface of the Venetian-Friulian plain consist of glaciofluvial sediments  
110 deposited during the considerable LGM aggradation phase, which in the Alps corresponds to the late  
111 Würm climate-stratigraphic unit (Chaline and Jerz, 1984) with the basal boundary at 35 ka cal BP  
112 (Spötl et al., 2013). These deposits formed fan-shaped alluvial features, properly called fluvial  
113 megafans (Fontana et al., 2008; 2014, Fig. 1).

114 Some high-quality deep boreholes drilled in the framework of different geological and  
115 geomorphological studies (Fontana et al., 2010a), allowed to investigate pre-LGM deposits and,  
116 specifically, to reach the sediments related to the penultimate glacial culmination, corresponding to  
117 the MIS 6 (Martinson et al., 1987). The top of these deposits is found at 70-45 m asl north-east of  
118 Venice while south-west its depth is comprised between 100 and 80 m asl (Massari et al., 2004; Pini  
119 et al., 2009; Fontana et al., 2010b).

120 The study area lies in the distal fine-grained sector of the megafan formed by the Brenta River (Mozzi  
121 et al, 2010, 2013).

122 The Middle and early Late Pleistocene stratigraphy of the area is poorly known, due to the lack in  
123 detailed stratigraphic studies deriving from the scarcity of deep cores available. Nevertheless, some  
124 valuable stratigraphic and paleontological information derived from two deep boreholes drilled in the  
125 thirties and fifties in the area of Padova (Accordi, 1950; Dieni and Proto Decima, 1960).

126 During the last 30 ka, the Brenta megafan experienced dramatic depositional changes in response to  
127 major climatic and environmental variations (Mozzi, 2005; Mozzi et al., 2013; Fontana et al., 2008  
128 and 2010a; Rossato et al., 2018). A dominant depositional trend occurred during the aggradation  
129 phase of the LGM (26.5 – 17.5 cal ka BP), with sedimentation rates up to 3 m/ka (Rossato and Mozzi,

130 2016), that was followed by a sharp erosive phase during deglaciation at around 17.5 ka. This latter  
131 led to the cutting of incised valleys, subsequently filled by Late Glacial and Holocene deposits (Iliceto  
132 et al., 2001; Mozzi, 2005; Mozzi et al., 2010, 2013; Cucato et al., 2012; Ninfo et al., 2016).

133

### 134 **3. Materials and Methods**

135 We explored the suitability to paleoecological, paleontological and stratigraphic analysis of two deep  
136 boreholes drilled in the Brenta River megafan: the 130 m-long GER1 and the 103 m-long CB  
137 boreholes. Drilling sites are located in the Padova city center at 13 m asl and 15 km south of Padova  
138 at 4.2 m asl, respectively (Fig 1). Both the boreholes were drilled through continuous rotary drilling  
139 method. The recovery was almost total for both the core (about 98-99%), but about 15% of CB  
140 sediments were reworked.

141 We adopted a multidisciplinary approach to the study of the cores' stratigraphy and correlations,  
142 analyzing different proxies to allow the recognition of sedimentary environments, climatic and  
143 environmental conditions. The following proxies have been considered:

- 144 - lithofacies and their assemblages;
- 145 - major unconformities (soils and erosional surfaces);
- 146 - pollen and non-pollen palynomorphs (NPPs) content;
- 147 - macro- and micropaleontological content.

148 Radiocarbon dating was used to constrain the chronology of the upper parts of both cores.

149

#### 150 **3.1 Lithofacies analysis**

151 Both stratigraphic successions were studied in detail through the macroscopic observation of the  
152 deposits. Different lithofacies were recognized based on grain size (Udden-Wentworth scale - Udden,  
153 1914; Wentworth, 1922) and considering other sedimentological features such as sedimentary  
154 structures, distribution trend, fossil content, bioturbation, organic content, unconformities and

155 paleosoils. The simplified lithostratigraphic description of the cores is reported in the stratigraphic  
156 logs (Fig. 2).

157 The paleosoils were described according to Jahn et al. (2006), based on the soil texture, color (Munsell  
158 Soil Color Charts), reaction to HCl 10% solution on a four-degree scale, and the presence of hard and  
159 soft carbonate concretions (Tab. 1). In order to allow comparison between different stages of soil  
160 development, the paleosoils were grouped in three classes as follows, using evidence of vertical  
161 carbonate leaching and precipitation along the soil profile: poorly developed, moderately developed,  
162 well developed.

163 The combined analysis of the lithofacies and main unconformities aimed at recognizing major  
164 stratigraphic units, as well as defining the different sedimentary environments.

165

### 166 **3.2 Pollen and NPPs analysis**

167 Peat intervals and fine-grained organic levels of both cores were systematically sampled for pollen  
168 analysis. 64 samples were processed for GER1 and 87 for CB (Fig. 2).

169 Preparation of samples followed standard methods (Faegri and Iversen, 1989), including HCl 10%,  
170 hot KOH 10%, sieving ( $\emptyset= 250 \mu\text{m}$ ), HF 39% (hot for GER1 samples; cold for 48 hours for CB  
171 samples), acetolysis and sieving ( $\emptyset= 10 \mu\text{m}$ ).

172 The amount of sediment treated per sample depends on the lithology: a volume of 1-3 cm<sup>3</sup> of organic-  
173 rich sediments, up to 10 cm<sup>3</sup> of organic poor-clay. *Lycopodium* spores were added to obtain estimates  
174 of palynomorph concentration per cm<sup>3</sup> of sediment according to Stockmarr (1971).

175 Identification was carried out under an optical microscope at a magnification of  $\times 400$ , using Moore  
176 et al. (1991), Beug (2004), Reille (1992 – 1995) and the reference collection of the Lab. of Palynology  
177 at University of Padova. NPPs were identified on the basis of specialized literature reviewed by Miola  
178 (2012); however, only foraminifers were considered in the discussion since the main aim was the  
179 paleoclimatic reconstruction.

180 The preservation of the pollen types was analyzed according to Huntley and Birks (1983) and  
181 Berglund (1986).

182 At least 200 pollen grains were identified for each sample (GER1: min 202, max 3075, av. 844; CB:  
183 min 219, max 1279, av. 656). The pollen samples where Upland pollen sum (Poaceae, *Alnus* and  
184 Cichorioideae, Hygrophytes, Hydrophytes and undetermined excluded) was less than 100 grains were  
185 not represented in the pollen diagrams. In these samples the Upland pollen concentration was  
186 generally less than 500 grains/ml.

187 The pollen percentages are based on trees, shrubs, upland herbs (including xerophytes) (PS), with the  
188 exclusion of *Alnus glutinosa* type and Poaceae. The abundance of these taxa is quite variable and  
189 probably over-represents plants growing in local sedimentary environments, thus biasing the general  
190 trend of % curves of regional vegetation taxa (Faegri and Iversen, 1989). Moreover, we decided to  
191 use this PS to compare our data with two reference pollen records from the same geographical area  
192 (Pini et al., 2009; 2010), where the same PS has been used as basis for the percentage calculation. For  
193 this reason, also Cichorioideae have been excluded from the PS. Percentage of *Alnus*, Poaceae,  
194 Cichorioideae, Hydrophytes, Hygrophytes, undetermined (degraded) pollen and each group of NPPs  
195 have been calculated on the basis of PS plus the counts of each group.

196 Pollen diagrams were drawn using the software *Tilia 2.6.1* (Grimm, 1991-2019) and Adobe Illustrator  
197 CC2018 for further graphical processing (Figs. 3, 4).

198

### 199 **3.3 Micropaleontological analysis**

200 21 sediment samples for foraminifera analysis were taken from GER1 core (Fig. 2). The samples,  
201 with weight ranging between 100 and 200g, were dried at 50°C and washed through a 0.063mm mesh  
202 sieve. The fraction >0.063mm was examined at stereomicroscope.

203 Regarding the samples processing from CB core, the reader is referred to Cucato et al. (2012).

204 Summarizing, 30 samples were washed in wet conditions, sieved through a 0.045 mm mesh sieve and

205 stored in a 50% ethanol-50% water solution. The smaller mesh was selected to check the presence of  
206 testatae amoebae.

207 The semi-quantitative analysis for foraminifera assemblages was carried out through a  
208 stereomicroscope (in wet conditions for the CB samples) at specific level for both the cores.

209

### 210 **3.4 Radiocarbon chronology (Tab. 1)**

211 The chronology of the upper 35 meters of both cores was investigated through the radiocarbon dating  
212 of peat samples (Fig. 2). The dated samples were extracted from the inner part of the cores and  
213 wrapped in aluminum foil to avoid contamination. AMS dating of bulk samples was performed at the  
214 AMS Laboratory, ETH Zürich for GER1 core and by the Tandem Laboratory, University of Uppsala  
215 for CB core.  $^{14}\text{C}$  ages were calibrated using the online radiocarbon calibration programme *OxCal*  
216 (version 4.3, calibration curve IntCal13; Bronk Ramsey, 2009). Tab. 1 summarizes the main  
217 information on the available radiocarbon chronology, i.e. dated levels and their provenance, type of  
218 material dated, lab code assigned to each sample, radiocarbon age and calibration.

219

## 220 **4. Results and Discussion**

221

### 222 **4.1 Lithostratigraphy and sedimentary environments**

223 The simplified lithostratigraphic logs of the sedimentary successions investigated in the GER1 and  
224 CB cores are reported in the Fig. 2.

225 Main stratigraphic units are outlined hereafter. The depths are relative to the ground surface.

226

#### 227 **4.1.1 Geriatrico 1 log (GER1)**

228 *Unit GER1 - I (130.00 – 118.65 m)*

229 The bottom part of the unit is a 0.40-m thick medium-fine sand layer with scattered mud clasts and  
230 pebbles. Above this layer and up to 119.30 the unit consists of medium-fine gravel with sandy matrix.  
231 Finally, a sharp transition to silty clay – clay levels with rounded pebbles is observed.

232 Interpretation: infilling of a fluvial channel, incised within the alluvial plain during a deglaciation  
233 erosive phase, in agreement with what observed at the end of LGM in the Venetian plain (Iliceto et  
234 al., 2001; Mozzi, 2005; Mozzi et al., 2010, 2013; Cucato et al., 2012; Ninfo et al., 2016).

235

236 *Unit GER1 - II (118.65 – 106.10 m)*

237 The bottom of the unit corresponds to the base of a 0.4-m thick peat level, one of the thickest in the  
238 whole succession. Above it, alternations of silty and silty clay occur, sometimes organic or peaty and  
239 bioturbated, and fine sand which shows thin lamination mainly toward the top.

240 The upper part is characterized by the presence of five poorly developed paleosoils (Soils 1-5 – GER1,  
241 Tab. 2).

242 Interpretation: proximal floodplain with frequent crevasse splays and a transition to lacustrine  
243 conditions toward the top. The presence of soils embedded in the succession indicates recurrent  
244 periods of floodplain stability.

245

246 *Unit GER1 - III (106.10 - 72.35 m)*

247 Mainly fine-medium sand with silty intercalations and frequent bioturbation and shell fragments until  
248 about 100 m depth, followed by about ten meters of alternations between predominant silty levels,  
249 often laminated and rich in plant remains, and fine sand with frequent peat intervals. Until the unit  
250 top, alternation between fine – medium sand and silt with frequent millimetric plant remains and  
251 common parallel and cross laminations. At the top, the unit has a 0.5 m thick peat level, the thickest  
252 one of the whole sedimentary succession.

253 A bi-sequential moderately developed paleosoil (Soil 6-GER1) is present between 73.80 and 74.90  
254 m depth (Tab. 2).

255 Interpretation: transition from an initial paralic environment such as a delta front, which evolves to  
256 delta and finally to alluvial plain conditions.

257

258 *Unit GER1 - IV (72.35 - 50.15 m)*

259 The unit bottom is represented by a sharp transition to medium-coarse sand, which is found as  
260 prevalent grain size until 63.00 m, in alternation with fine sand and silt.

261 Until the top, the sequence is characterized by the alternation between finer sediments with the  
262 prevalence of both sandy and clayey silt on fine sand and the presence of organic and peaty levels.

263 Between 50.40 and 50.15 m of depth frequent fresh-water shells fragments are found.

264 A well-developed soil (Soil 7-GER1) is found at the unit top (Tab. 2).

265 Interpretation: fluvial channel deposits with a transition to a proximal floodplain environment toward  
266 the top, within an aggrading alluvial plain.

267

268 *Unit GER1 - V (50.15 – 30.00 m)*

269 Mainly medium-fine silty sand with silty and clayey levels in the lower part of the unit, with a  
270 decrease of grain size and an increase of organic levels in the upper part. Here several peat intervals  
271 are present.

272 A bi-sequential moderately developed paleosoil (Soil 8-GER1) is found between 40.75 and 41.45 m  
273 of depth (Tab. 2).

274 An intercalation of organic carbonaceous matter in silt, sampled at 30.98 m of depth, yielded a  
275 radiocarbon age of  $40595 \pm 340$  cal a BP.

276 Interpretation: alluvial floodplain sediments, deposited in an environment characterized by common  
277 crevasse splays, less frequent toward the top.

278

279 *Unit GER1 - VI (30.00 – 13.65 m)*

280 Mainly fine - medium sand, sometimes laminated, with subordinate silt intercalation until 23.00  
281 meters depth, followed by an increase in silty fraction and the occurrence of several 3-4 cm thick peat  
282 levels.

283 Interpretation: transition from a fluvial channel with sandy bars to floodplain conditions characterized  
284 by sporadic swamping, within an aggrading alluvial plain.

285 A peat intercalation in organic fine sand, sampled at 20.80 m of depth, yielded an age beyond the  
286 limit of the  $^{14}\text{C}$  method and it is interpreted as reworked, whereas a peat sample collected at 14.08 m  
287 has been dated  $23187 \pm 260$  cal a BP.

288

289 *Unit GER1 - VII (13.65 – 2.35 m)*

290 Prevalent medium to coarse sand with common pebbles up to 2 cm. The base could be erosive and  
291 the upper part is composed by massive silt.

292 Interpretation: fluvial channel deposits, probably related to the infilling of a previous incised valley.

293

294 *Unit GER1 - VIII (2.35 – 0.00 m)*

295 Reworked anthropogenic fill.

296

#### 297 **4.1.2 Ca' Borille log (CB)**

298 *Unit CB - I (103.00 – 99.23 m)*

299 Mainly fine-medium sandy succession with intercalations of sandy and clayey silt, rarely peaty silt.  
300 Frequent wood remains and arenaceous concretions containing pyrite. Short fining-upward intervals  
301 are recognized.

302 Interpretation: predominant alluvial floodplain deposits, deposited in an environment characterized  
303 by frequent crevasse splays.

304

305 *Unit CB - II (99.23 – 85.62 m)*



306 Grey and grey-greenish sandy sediments with subordinated intercalations of silt, sandy silt and clay.  
307 Persistent presence of mollusk shell fragments until 87 m depth, concentrated into two levels of  
308 biocalcirudite (between 99.00 and 98.55 m) containing prevalent *Glycimeris*, *Tellina*, *Chlamis*,  
309 *Cardium* and subordinated gastropod shell fragments, arenaceous – silty concretions covered by  
310 bryozoa and serpulids, and rare wood remains. The clayey levels show evidence of bioturbation.  
311 Interpretation: proximal marine deposits pertaining to a succession evolving from a retro-barrier  
312 environment to shore-face conditions.

313

314 *Unit CBB - III (85.62 – 73.08 m)*

315 Fine sand to clay, often organized in fining-upward sequences. Several peat levels, with a maximum  
316 thickness of 0.25 m, are included in this unit. Frequent wood remains are present, mainly concentrated  
317 in the lower part of the unit. Toward the top some marine shell fragments with strong ornamentation  
318 (probably *Cardium*) occur. The entire unit is characterized by widespread bioturbation.  
319 Interpretation: delta plain deposits.

320

321 *Unit CB - IV (73.08 – 56.96 m)*

322 Medium-coarse sand to clay, with common presence of peat intervals in the lower part of the unit.  
323 The bottom of the succession corresponds to the base of a 0.9 m thick peat level, the thickest one all  
324 along the succession. Other thinner peat intervals are found up to 68.00 m depth, while they are absent  
325 in the upper part of the unit.  
326 A major erosive surface, representing the base of a channel body, is found at 60.50 m depth. The  
327 channel body is characterized by medium-coarse sand passing upward to fine sand with silt and clayey  
328 silt intercalations. The unit top is marked by a sharp passage from fine sand to clay with evidence of  
329 load deformation structures.

330 Interpretation: floodplain deposits with the establishment of a fluvial channel. The lower part of the  
331 unit can be attributed to an area distant from the river, where wetlands could develop. The middle

332 part of the unit corresponds to proximal floodplain conditions with abundant crevasse splay deposits,  
333 followed by the establishment of a channel body with sandy sedimentation.

334

335 *Unit CB - V (56.96 – 50.67 m)*

336 Mainly grey and grey-greenish clay and organic clay successions, sometimes organic, with thin  
337 parallel lamination. Sporadic presence of thin silt laminations between 56.00 and 55.00 m and toward  
338 the unit's top. Some peat intervals are found between 53.00 and 52.00 m. A moderately developed  
339 paleosoil (Soil 1-CB) is found between 50.60 and 52.00 m (Tab. 2).

340 Interpretation: lacustrine conditions evolving to wetland and finally to floodplain conditions.

341

342 *Unit CB - VI (50.67 – 31.50 m)*

343 The unit starts with a sharp transition to medium sand and it is characterized by cyclical grain size  
344 variations, with recurrent fining upward sequences with a medium or fine sandy base evolving to  
345 sandy silt, silt and clay or peat toward the top. Wood remains are frequent, mostly concentrated in the  
346 peat and organic clay levels.

347 A moderately developed paleosoil (Soil 2-CB) is found between 49.55 and 50.00 m of depth (Tab.  
348 2). A peat sample collected at 33.54 m of depth has provide an age beyond the radiocarbon dating  
349 method.

350 Interpretation: alluvial plain deposits pertaining to a succession with recurrent transition between  
351 channel and overbank floodplain conditions.

352

353 *Unit CB - VII (31.50 – 17.64 m)*

354 Mainly medium sand with subordinate coarse sand and fine sand intercalation until 26.00 m, followed  
355 by prevalent fine sand with silt. Toward the top, organic silt and peat intervals occur. An erosive  
356 surface represents the unit bottom.

357 A peat sample collected at 17.70 m of depth yielded a radiocarbon age of 25201 ± 585 cal a BP.

358 Interpretation: these sediments represent the transition from a fluvial channel with sandy bars to  
359 floodplain conditions characterized by sporadic marsh conditions.

360

361 *Unit CB - VIII (17.64 – 2.55 m)*

362 The unit starts with a transition from peaty silt to fine sand and it is divided in 3 successions:

- 363 - 8a (17.64 – 12.94 m): parallel cross-laminated fine-medium sand with increasing silt  
364 laminations toward the top. At the top, a 7 cm thick silty clay, sometimes organic, layer is  
365 present with several plant remains and terrestrial gastropod shells (*Planorbis*);
- 366 - 8b (12.94 – 9.40 m): alternation between fine sand/silty fine sand and predominant silt or  
367 organic silt;
- 368 - 8c (9.40 – 2.55 m): predominance of silt and clay with peaty intercalations.

369 A well-developed paleosoil with gley pedofeatures (Soil 3-CB) is found between 2.90 and 3.60 m of  
370 depth (Tab. 2). A peat sample collected at 7.52 m of depth yielded a radiocarbon age of  $21194 \pm 505$   
371 cal a BP.

372 Interpretation: the lowermost sediments are interpreted as the result of a transition from a fluvial  
373 channel with sandy bars to levee's facies and, finally to low energy floodplain conditions (8a). The  
374 interpreted depositional environment of the middle part (8b) is a proximal floodplain with common  
375 crevasse splays, whereas in the upper part (8c) distal floodplain conditions are documented.

376 The paleosoil within succession 8c formed in poorly drained soil conditions.

377

378 *Unit CB - IX (2.55 – 0.00 m)*

379 Silty – clayey sediments affected by modern soil development (Soil 4-CB, Tab. 2).

380 Interpretation: distal floodplain deposits, documenting well developed soil formation relative to the  
381 present topographic surface. Due to pedogenic processes, the upper horizon (now partly destroyed by  
382 plowing) suffered from carbonate leaching, while in the lower ones an enrichment in calcium  
383 carbonate is found as Bk horizon.

384

## 385 **4.2 Micropaleontological results**

386 In GER1 core foraminifera were present only in 6 samples (104.65-104.75, 103.90-103.95, 98.75-  
387 98.80, 92.65-92.70, 82.30-82.35, 80.85-80.90), and they were only benthonic. Although the  
388 foraminiferal assemblages present in CB core were already reported in Cucato et al. (2012), it is  
389 worthy to remind that among the 30 analyzed samples only two, positioned in the lower part of the  
390 borehole (97.82 and 98.44m) contained foraminifera, again only benthonic.

391 For a more complete view, two biofacies (A and B) and an additional facies (C), without any biosome  
392 or bioclast, are distinguished and described below, which best reflect the content of all the examined  
393 samples of the two cores.

394

395 *Biofacies A1 (GER1 104.65, 103.90, 98.75, 92.65, 82.30, 80.85 m)*

396 The samples contain abundant fine sand along with plant remains, shell remains (ostracods) and  
397 bioclasts. *Ammonia beccarii tepida* is the most common species, accompanied by *Elphidium*  
398 *granosum*, and by sporadic specimens of *Ammonia beccarii*, *Quinqueloculina seminulum*, *Ammonia*  
399 *papillosa*, *Elphidium decipiens*, *Haynesina germanica*, *Rosalina globularis*, and *Elphidium advenum*.  
400 This biofacies may be referred to a transitional environment/lagoon.

401

402 *Biofacies A2 (CB 98.44 and CB 97.82 m)*

403 Foraminifers are not rare, although scattered within micaceous very fine sand and/or plant remains  
404 and in some case (CB 97.82 m) broken or blackened. Miliolids (*Quinqueloculina oblonga*, *Adelosina*  
405 *longirostra*, *Q. seminulum*, *Triloculina trigonula*, *Cornuspira involvens*) are common along with *E.*  
406 *advenum*, accompanied by *Ammonia perlucida*, *A. beccarii*, *R. globularis*, *Asterigerinata mamilla*,  
407 *Buccella granulata*, *Elphidium granosum* and rare specimens of *H. germanica*. This biofacies,  
408 suggests a very shallow marine environment (near-shore area, < 20-25 m water depth) and it can be  
409 equated to the biofacial unit II by Jorissen (1987). Indeed, this latter occupies the zone between 7.5

410 and 25 m depth with substrata generally coarse, rich in Ca carbonate, poor in organic matter and  
411 characterized by a benthonic foraminiferal assemblage mainly composed by *A. beccarii beccarii*, *A.*  
412 *beccarii tepida*, *E. advenum*, *Ammonia perlucida*, *A. longirostra*, *E. granosum*, *E. decipiens*, *T.*  
413 *trigonula*, *Nonion depressulum*. However, the presence of a prairie cannot be rule out in the  
414 paleoenvironment of the examined samples, because of the presence of the epiphytic taxa *A. mamilla*,  
415 *R. globularis* and *B. granulata*.

416

417 *Biofacies B (CB 12.90, 11.35, 10.62, 8.41 m and GER1 108.30 m)*

418 Foraminifera are absent, but scattered remains of other organisms (ostracods, otoliths, gastropods  
419 such as Planorbidae or *Hydrobia* spp) are present up to common. The samples show scarce presence  
420 of very fine sand while plant remains are in some case abundant. This biofacies may suggest a  
421 transitional to continental environment with low salinity/fresh water, and it can be ascribed to the  
422 interval 8.40-12.90 m in core CB and to the sample 108.30 m in core GER1.

423

424 *Facies C1 (GER1 98.20, 97.10, 95.60, 94.00, 93.60, 91.50 m and CB 85.45, 82.84, 77.82, 75.60,*  
425 *52.10, 49.10, 37.06 m)*

426 This facies includes samples presenting abundant (or only) plant remains. Very fine sand is scarce.  
427 Samples with this content could reflect both marine/transitional and freshwater environments.

428

429 *Facies C2 (GER1 109.73, 105.75, 103.30, 102.25, 100.20, 94.65, 78.67, 78.25 m and CB 91.42,*  
430 *100.84, 92.90, 85.80, 80.85, 75.36, 64.60, 62.28, 56.10, 54.85, 52.40, 31.90, 31.63, 31.60, 7.80,*  
431 *7.21, 5.50, 2.70 m)*

432 The samples are composed by very fine sand (in some case with oxidized clasts), scarce or absent  
433 plant remains, no foraminifera and very rare (frequently absent) small shell fragments. The samples  
434 of this facies, barren in fossil remains, may suggest a continental/fluvial environment.

435

436 **4.3. Palynological results**

437 Selected percentage pollen records from both the cores are shown in Figs. 3 and 4, whereas the  
438 complete pollen diagrams are supplied as supplementary materials (Supplementary materials 1 and  
439 2).

440 The preservation of pollen grains was often modest with high percentage of undeterminable grains  
441 (up to 50%, mainly broken saccate) for both the cores. Only 34 samples of GER1 core and 67 samples  
442 of CB core yielded a statistically significant (>100 grain/g) pollen sum (PS). The pollen spectra with  
443 a lower sum were considered sterile and excluded from the diagrams.

444 On the basis of the pollen assemblage of terrestrial plants, which give an indication of the regional  
445 vegetation, the pollen records were subjectively divided in zones, referring also to the stratigraphic  
446 data (see Section 4.1 and Fig. 2). The supplementary materials 3 and 4 report the percentage ranges  
447 and limits in table, facilitating the distinctions of pollen zones. Whilst in GER1 10 pollen zones were  
448 identified, 14 were determined in CB. In both cores the zones numbering increases toward the top.

449 The reconstruction of the regional vegetation and local plant communities of each core is summarized  
450 hereafter.

451

452 **4.3.1 Geriatrico 1 core (GER1)**

453 Due to the large number of sterile levels (30 samples out of 64 analysed samples) and the widespread  
454 occurrence of not analysed sandy layers (Fig. 2 and Tab. 2), the specific limits of the 10 pollen zones  
455 are based both on the pollen associations and the stratigraphic information (Section 4.1.). Moreover,  
456 large portions of the core are unfortunately devoid of pollen data (Fig. 3, supplementary material 1,  
457 3). Hereafter we present a description of pollen zones, with indications of their stratigraphic  
458 boundaries and reconstructed regional and local vegetations. For some pollen zones, correlations with  
459 zones identified in other pollen records from the same region are proposed.

460

461 *Zone GER1.1 (117.70 - 118.65 m) - Temperate mixed forest*

462 Arboreal pollen (AP) is represented by thermophilous and mesophilous broadleaved trees with  
463 prevalent *Quercus* undiff., *Carpinus betulus*, *Tilia*, *Fraxinus* undiff. and *Fagus*. Other deciduous trees  
464 such as *Pterocarya*, *Ulmus/Zelkova*, *Zelkova*, *Carya* and *Betula* are present. Conifers are less  
465 represented, however *Pinus*, *Abies* and *Picea* are continuously recorded.

466 Among the sporadic taxa the occurrence of *Buxus*, present only here and in the GER1.5 pollen zone,  
467 stands out. Moreover, among non-arboreal pollen (NAP), to be reported is the co-occurrence of  
468 Chenopodiaceae and *Limonium*, which may testify to the presence of salt marshes, and the continuous  
469 presence of *Artemisia*. Hygrophytes, Hydrophytes and Polypodiaceae occur.

470

471 *Zone GER1.2 (117.20 - 117.70 m) - Pinus forest with Picea and rare broad-leaved trees*

472 AP reaches here its lowest percentage, however it is dominant on NAP. *Pinus* is the most represented  
473 taxon followed by *Picea*, whereas decreasing values of *Abies* and increasing values of *Betula* are  
474 recorded toward the top. Broad-leaved trees are less abundant if compared with the previous zone  
475 and mostly represented by *Quercus*, *Corylus* and *Tilia*.

476 Xerophilous/halophilous NAP elements are continuously present and represented by *Artemisia*,  
477 Chenopodiaceae and deteriorate, probably reworked, *Limonium*, with a peak at 117.32 m depth.  
478 Hygrophytes and Hydrophytes are also present.

479

480 *Zone GER1.3 (99.30 - 100.50 m) - Mixed forest dominated by Pinus*

481 This zone is separated from the previous one by 16.71 m of sediments; no pollen grains were found  
482 in 12 samples from the interval 114.75 - 105.48 m depth.

483 The zone is represented by only one sample (100.00 m) with an AP assemblage constituted by *Pinus*  
484 for half. *Fagus*, *Betula*, *Pterocarya*, *Abies* and *Carpinus betulus* are present, whereas thermophilous  
485 trees are well represented by *Quercus* and *Tilia*. Among NAP, Hygrophytes and Polypodiaceae are  
486 common whereas Hydrophytes, Poaceae, *Senecio* type and *Hypericum* are present with low  
487 percentages.

488

489 *Zone GER1.4 (93.95 - 99.30 m) - Temperate broad-leaved forest with subordinate conifers*

490 AP is heterogeneous and dominated by taxa of broad-leaved trees. Thermophilous trees are common  
491 with *Quercus*, *Ulmus/Zelkova*, *Corylus*, *Tilia* and *Fraxinus*. *Carpinus betulus* is continuously  
492 recorded and a distinct peak of *Fagus* occurs at 97.80 m depth. *Pinus* is always present with  
493 percentages ranging from 20% to 50%, whereas *Picea* occurs only at the bottom of the zone. The  
494 highest value of *Pinus* is record at 97.6 m depth along with *Betula*. Among the herbs, *Artemisia*  
495 occurs. Polypodiaceae are abundant whereas Poaceae, Hygrophytes and Hydrophytes are quite  
496 common. *Senecio* type, *Hypericum*, *Helleborus* undiff, *Saxifraga hirculus* and other herbs are rare or  
497 sporadic.

498

499 *Zone GER1.5 (72.35 – 93.95 m) - Temperate broad-leaved forest with common conifers*

500 The zone includes seven sterile samples and some sandy levels which lack pollen information (e.g.,  
501 75.34 – 78. 54; 83.16 – 88.39 m).

502 The zone is dominated by thermophilous trees pollen which reach a distinct peak at 88.40 m depth.  
503 In respect to the prevoius zone, mesophilous taxa are more abundant with the continuous presence of  
504 *Fagus* and increased values of *Carpinus betulus*. *Abies* occurs, with values < 9%, and increased values  
505 of *Pinus* and *Picea* are recorded. *Betula* is still present with similar abundance. Among the sporadic  
506 taxa, *Buxus* occurs with very low percentage. Among the herbs Chenopodiaceae appear, whereas  
507 *Artemisia* percentage slightly increases.

508 Poaceae, Hygrophytes and Polypodiaceae are abundant. Other herbs are *Saxifraga hirculus* typ,  
509 Brassicaceae and *Senecio* type.

510

511 *Zone GER1.6 (54.95 - 57.40) - Pinus forest and steppic plant communities of cold and dry climate*

512 14.95 m of not analysed silt-sand layers separate this zone from the previous one.



513 The zone is represented by only one sample (57.36 m) because of the presence of four sterile samples  
514 (56.77, 56.36, 56.19, 55.65 m). Pollen concentration is low and the AP assemblage quite entirely  
515 represented by *Pinus* with low values of *Betula*. Pollen of broad-leaved thermophilous trees is absent.  
516 The zone records a climatic cooling and a dryness increasing, as testified by the absence of  
517 thermophilous and mesophilous trees and the presence of xerophytic herbs and shrubs (*Artemisia*,  
518 *Ephedra fragilis* type, Chenopodiaceae). Other common herbs are Poaceae and Hygrophytes.

519

520 *Zone GER1.7 (43.40 – 45.40 m) - Temperate broad-leaved forest with Pinus, gradually evolving to*  
521 *more open condition*

522 The zone is separated from the previous one by 9.55 m of prevalently silty-sandy layers. Two samples  
523 from organic clayey levels were collected at 54.56 and 52.05 m and yielded no pollen.

524 AP is heterogeneous with abundant *Pinus* and well represented mixed deciduous trees. The zone is  
525 characterized by a constantly decreasing values of *Pinus*, *Quercus*, *Fagus*, *Carpinus betulus* and  
526 *Ulmus/Zelkova* toward the top, whereas *Corylus*, *Tilia*, *Picea* and *Abies* remain stable and  
527 Hygrophytes increase. Although with low percentages, Poaceae, *Artemisia* and Brassicaceae are  
528 present, as well as Hydrophytes.

529

530 *Zone GER1.8 (37.40 – 37.90 m) - Open pine-birch forest with temperate elements and steppic plant*  
531 *communities of cold and dry climate*

532 Two sample (42.12, 41.34 m), collected in the 5.5 m thick interval separating this zone from the  
533 previous one, are sterile.

534 AP assemblage is rich of *Pinus* with abundant *Betula* and rare *Picea*. Few temperate deciduous trees  
535 (*Quercus*, *Tilia*, *Fagus*, *Carpinus betulus*, *Castanea sativa*) occur with low abundance.

536 Xerophytic herbs are well represented by the co-occurrence of *Artemisia* and Chenopodiaceae, along  
537 with sporadic grains of *Senecio* type, *Apiaceae*, *Valeriana officinalis* type, Hydrophytes and others.

538 Hygrophytes are common and Polypodiaceae occur with low percentage.

539

540 *Zone GER1.9 (30.00 – 34.87 m) - Open pine-birch forest with steppic plant communities of cold and*  
541 *dry climate*

542 This zone is separated from the previous one by 2.53 m of not analysed silt and sand.

543 AP values ranges between 65 and 90%, mostly represented by *Pinus*, *Juniperus*, *Betula* and *Picea*.

544 Pollen of broad-leaved thermophilous and mesophilous trees is very rare and represented by few

545 grains of *Carpinus betulus*, *Corylus*, *Quercus*, *Tilia* and *Cornus sanguinea*. Xerophytic herbs and

546 shrubs are abundant with *Artemisia*, *Chenopodiaceae* and *Ephedra fragilis* type. Poaceae and

547 Hygrophytes are also common, whereas Polypodiaceae are poorly represented. *Senecio* type,

548 *Valeriana officinalis* type, *Saxifraga aizoides* type and Hydrophytes are rare.

549

550 *Zone GER1.10 (13.97 – 14.40 m) - Steppe and xerophytic scrubs with conifer grooves*

551 15.60 m of not analysed silt and sand separate this zone from the previous one.

552 The zone is represented by only one sample (13.98 m). The percentage of AP is relatively low (70%-

553 80%) and dominated by *Pinus* but with lower values of *Juniperus*, *Betula* and *Picea* in respect to the

554 previous zone. Xerophytic herbs and shrubs are still abundant with *Artemisia*, *Ephedra fragilis* type,

555 *Chenopodiaceae* and *Valeriana officinalis* type. *Senecio* type is sporadic. Hygrophytes are common.

556

#### 557 **4.3.2 Cà Borille core (CB)**

558 Due to the higher pollen concentration and lower number of sterile samples (26 samples out of 87

559 analyzed samples), the lower occurrence of wide sandy portions not analysed (Fig. 2) and the

560 consequent major sampling concentration (61 samples in 103 m), this core allowed to distinguish 14

561 pollen zones in a more continuous way in comparison to GER1 core (Fig. 4, supplementary material

562 2, 4). However, the limits between the zones are defined both on stratigraphic and palynological data.

563

564 *Zone CB1 (99.23 – 103.00 m) - Pinus forest with xerophilous elements*

565 The zone is represented by only one sample (102.03 m) because of the presence of three sterile  
566 samples (102.05, 99.09, 99.05 m). AP assemblage is almost completely constituted by *Pinus* and  
567 unidentified broken saccate. Sporadic grains of *Picea* and *Fagus* occur. NAP is represented by  
568 Poaceae, xerophytic elements, Apiaceae and Hydrophytes.

569

570 *Zone CB2 (98.70 - 99.23 m) – Open temperate broad-leaved forest*

571 The AP assemblage reaches the lowest values of the whole core and is dominated by *Carpinus betulus*  
572 with subordinated *Quercus*, *Corylus*, *Cornus mas* and *Pinus*. Other mixed elements such as *Abies*,  
573 *Picea*, *Fagus*, *Ulmus*, *Salix*, *Fraxinus*, *Tilia* and *Acer* are sporadically present. NAP is principally  
574 represented by Chenopodiaceae, which co-occur with other xerophilous/halophilous taxa such as  
575 *Artemisia*, Asteraceae Cichorioideae and *Limonium*. Poaceae are also common, whereas Hygrophytes  
576 and Hydrophytes are rare.

577

578 *Zone CB3 (80.92 - 85.62 m) - Temperate mixed forest*

579 This zone is separated from the previous one by 13.08 m of not analysed sandy layers.  
580 With the exception of the sample at 83.18 m depth where AP is about 30%, AP is higher than in the  
581 previous zone and is dominated by *Quercus* in the lower part, *Carpinus betulus* in the middle and  
582 *Fagus* in the upper part of the zone. Other thermophilous trees and shrubs such as *Corylus* and *Ulmus*  
583 are common, whereas the conifers are poorly represented although continuously present, in particular  
584 *Pinus* percentage does not exceed 20%. Among the rare taxa, *Buxus* is recorded. NAP is represented  
585 by a very high variety of taxa; the most common are Hygrophytes, Poaceae, Apiaceae, *Aster* type,  
586 *Sinapis* type (Brassicaceae), Labiatae A group. The pollen assemblage of the sample at 83.18 m is  
587 dominated by Chenopodiaceae, Poaceae and *Limonium*. Among AP assemblage, *Carpinus betulus* is  
588 dominant with subordinated *Quercus*, *Corylus* and *Fagus*.

589

590 *Zone CB4 (76.94 - 78.26 m) - Open pine-birch forest with residual stands of temperate broad-leaved*  
591 *trees*

592 A layer of 2.66 m of sands separate this zone from the previous one.

593 The zone includes four sterile samples (78.24, 78.14, 77.91, 77.79 m). The pollen assemblage of the  
594 unique sample (77.66 m) is mainly constituted by Poaceae.

595 AP is represented by *Pinus*, *Betula* and subordinated *Picea*. Sporadic *Quercus* and *Fagus*, rare  
596 *Carpinus betulus* and *Tilia* are also present.

597

598 *Zone CB5 (71.57 - 76.94 m) - Temperate broad-leaved forest*

599 AP is mostly represented by temperate broad-leaved trees with *Quercus* followed by *Fagus*, *Carpinus*  
600 *betulus*, *Corylus* and *Ulmus* slightly decreasing from the middle toward the top of the pollen zone.

601 Conifers are poorly but continuously present whereas *Betula* appears at the top, where *Pinus* and  
602 broken saccate are more abundant. Among the rare and sporadic taxa, the presence of *Buxus* and *Vitis*  
603 *vinifera* stands out.

604 NAP is dominated by Poaceae with common Chenopodiaceae. At 74.42 m the rare presence of  
605 *Limonium* is recorded in correspondence with Dinoflagellates and IOLs of foraminifers.

606 This zone presents some similarities with the pollen zone AZ51 of the AzzanoX core in which an  
607 open broad-leaved forest with dominant deciduous *Quercus* with *Fagus* and scattered conifers is  
608 recorded. That interval is moreover characterized by the presence of pollen types of salt marshes (Pini  
609 et al., 2009).

610

611 *Zone CB6 (67.70 - 71.57 m) - Conifer forest with birch and residual stands of temperate broad-leaved*  
612 *trees*

613 AP is mainly constituted by *Pinus* and broken saccate whose abundance vary irregularly along the  
614 zone. *Abies*, *Picea* and *Betula* are also common and more abundant than temperate broad-leaved trees  
615 and shrubs (*Fagus*, *Carpinus betulus*, *Corylus*, *Cornus mas*, *Ulmus*, *Fraxinus*), which decrease

616 toward the top of the zone. Rare grains of *Olea europaea* occur at 70.40 m depth. Among NAP,  
617 Poaceae are abundant and followed by *Artemisia*, whose percentage increases upward. Other herbs  
618 are Hygrophytes, Apiaceae, Chenopodiaceae, *Sinapis* type (Brassicaceae).

619

620 *Zone CB7 (60.49 - 61.13 m) - Pinus forest and steppic plant communities of cold and dry climate*

621 This zone is separated from the previous one by 6.57 m of prevalent sandy layers. Four samples within  
622 this interval were sterile (65.00, 64.54, 62.30, 61.15 m).

623 The zone includes two samples with AP almost completely constituted by *Pinus* and broken saccate.

624 *Picea* and *Betula* are present with low percentage. Very rare are thermophilous trees. NAP is not well  
625 represented, including Hygrophytes and Poaceae with subordinated xerophytic herbs such as  
626 *Artemisia* and Chenopodiaceae. The pollen assemblage may be correlated to zones AZ53-54 of  
627 AzzanoX core which are referred to a phase of cool and dry climate (Pini et al., 2009). Moreover, this  
628 zone is very similar to the GER1.6 zone.

629

630 *Zone CB8 (50.67 - 52.55 m) – Temperate broad-leaved forest*

631 This zone is separated from the previous one by 7.94 m of sediments devoid of pollen information:  
632 between 56.96 and 60.49 m of depth sandy layers occur and between 55.13-53.74 m depth 4 samples  
633 yielded very low pollen sums.

634 The zone is characterized by AP dominated by thermophilous and mesophilous broad-leaved trees  
635 and shrubs such as *Carpinus betulus*, *Quercus*, *Ulmus*, *Corylus*, *Cornus mas* and others. Conifers are  
636 continuously present, although with low percentage increasing toward the top. *Buxus* reaches the  
637 highest value of the core in this zone (10%), *Fagus* does not exceed 2%, and rare grains of *Olea*  
638 *europaea* are recorded between 52.04 and 51.94 m of depth. NAP presents a great variety of taxa, the  
639 most represented are Poaceae, Hygrophytes, *Artemisia*, Apiaceae and Chenopodiaceae.

640 The zone presents similarities with the pollen zone AZ55 of AzzanoX core which is referred to a  
641 broad-leaved thermophilous forest under interglacial climate conditions, with dominant *Quercus* and

642 rare *Fagus* (Pini et al., 2009). The presence of *Buxus* and *Olea europaea* in the frame of a mixed  
643 forest with abundant *Carpinus betulus* and *Quercus* recalls the FDP 11d-f zones of Fimon – Ponte  
644 sulla Debba core (Pini et al., 2010).

645

646 *Zone CB9 (45.73 - 46.00 m) - Pinus forest with scattered Picea and xerophytic elements*

647 This zone is separated from the previous one by 4.67 m of sediment that provide two sterile samples  
648 (49.96, 47.25 m), and is constituted by only one sample (45.81 m).

649 AP is represented by *Pinus* and abundant broken saccate with *Picea* and few grains of *Abies*. Broad-  
650 leaved trees and shrubs are still present, although with lower abundance in respect to the previous  
651 zone, with the exception of *Fagus* and *Tilia* which are more abundant. NAP is represented by Poaceae  
652 with *Artemisia* and Chenopodiaceae. The zone is constituted by only one sample; the pollen spectrum  
653 might reflect colder and dryer climatic conditions, similar to those recorded in the pollen zone AZ57  
654 of the AzzanoX core (Pini et al., 2009) as well FDP 11g-12 zone of Fimon – Ponte sulla Debba core  
655 (Pini et al., 2010).

656

657 *Zone CB10 (41.68 - 45.73 m) - Temperate mixed forest*

658 AP is mainly represented by thermophilous and mesophilous broad-leaved trees and shrubs with  
659 dominant *Carpinus betulus* followed by *Quercus*, *Fagus*, *Ulmus*, *Corylus* and *Tilia*. Among the  
660 conifers, *Picea* and *Pinus* are the most represented, although with low percentage, followed by *Abies*.  
661 NAP shows great heterogeneity of upland herbs with dominant Poaceae as well as common Hygro-  
662 and freshwater Hydrophytes. The presence of quite abundant *Fagus* and the absence of *Buxus*, are  
663 the main remarkable differences with the CB8 zone. These features, in addition to the occurrence of  
664 the sequence CB8-CB9 suggest a comparison with the pollen zone AZ59 of the AzzanoX core (Pini  
665 et., 2009), even if the latter records higher percentage of *Pinus*. However, the presence of temperate  
666 taxa and the expansion of *Fagus* are coherent. Similarly, the zone recalls the upper part of the

667 superzone FDP 13 of Fimon – Ponte sulla Debba core (Pini et al., 2010), although *Picea* and *Abies*  
668 are in this last record better represented.

669

670 *Zone CB11 (40.00 - 41.68 m) - Open pine forest with Picea and xerophytic scrubs*

671 AP shows values < 70% and toward the top of the zone, it is subordinate to NAP. It is constantly  
672 dominated by *Pinus* with abundant broken saccate and common *Picea*. Temperate taxa are almost  
673 completely absent. NAP is dominated by Poaceae and *Asteraceae* undiff. with a great variety of less  
674 represented upland herbs taxa. Hydro- ad Hygrophytes are present with low percentage values. At the  
675 depth of 40.01 m a peak of Chenopodiaceae and *Limonium* is recorded along with rare foraminifers.  
676 A remarkable percentage of undetermined pollen occurs here, due to pollen preservation issues.

677 Despite the absence of *Betula*, this pollen assemblage recalls the AZ61 and FDP14 zones of the  
678 AzzanoX and Fimon – Ponte sulla Debba cores (Pini et al., 2009; 2010), which documents a forest  
679 withdrawal and the expansion of herbaceous steppic and xerophilous elements.

680

681 *Zone CB12 (33.52 - 40.00 m) - Mixed broad-leaved forest with Picea*

682 AP ranges between 40% and 90% and is mainly represented by broad-leaved trees and shrubs.  
683 *Quercus*, *Carpinus betulus* and *Ulmus* are co-dominant and followed by *Fagus*, *Corylus* and *Tilia*.  
684 *Pinus* and *Picea* are quite well represented, whereas *Betula* is scarcely present as well as *Abies*.  
685 Among rare taxa, *Castanea sativa* and *Vitis vinifera* are recorded. NAP is mainly represented by  
686 Poaceae and Hygrophytes. A peak of *Aster* type with Chenopodiaceae and *Limonium* is recorded at  
687 the bottom of the zone.

688 The zone presents some similarities with AZ62 zone of AzzanoX core (Pini et al., 2009), except for  
689 the low *Betula* occurrence, with the FDP15a zone of Fimon – Ponte sulla Debba core (Pini et al.,  
690 2010) and the Rugo5 zone of the Valeriano Creek succession (Monegato et al., 2010).

691

692 *Zone CB13 (31.50 - 33.52 m) - Open pine forest with steppic plant communities of cool and dry*  
693 *climate*

694 AP is almost completely constituted by *Pinus* and broken saccate with *Betula* and *Picea*. Temperate  
695 trees are almost completely absent with the exception of *Tilia* and extremely rare grains of *Carpinus*  
696 *betulus* and *Quercus*.

697 NAP is dominated by Poaceae and Hygrophytes with few taxa of xerophilous herbs.

698 The cold pollen assemblage with the presence of reduced warm temperate taxa and the persistence of  
699 *Tilia* up to 5%, recalls the FDP16a zone of Fimon – Ponte sulla Debba core (Pini et al., 2010a).

700

701 *Zone CB14 (7.35 – 25.05 m) - Open pine-birch forest with plant communities of cool and dry climate*

702 This zone is separated from the previous one by 6.45 m of not analysed medium-coarse sand.

703 AP is mainly constituted by *Pinus*, broken saccate, and *Betula*. *Corylus* and *Picea* sporadically occur  
704 whereas other temperate taxa such as *Tilia*, *Cornus sanguinea* and *Quercus* are extremely rare in the  
705 lower part of the zone. Among NAP, Poaceae, *Artemisia*, Chenopodiaceae, Apiaceae and *Aster* type  
706 are well represented. Hygrophytes are also present. The overall abundance of *Pinus*, grasses and  
707 xerophytes with the low persistence of thermophilous trees and shrubs recalls the AZ68 zone of  
708 AzzanoX core where the sporadic presence of temperate taxa is related to long-distance transport or  
709 to reduced refugial populations (Pini et al., 2009). Similar features are recorded in GER1.10 zone.

710

## 711 **5. Correlation between GER1 and CB cores, climate stratigraphy and landscape reconstruction**

712 Information retrieved from palaeoecological records are relevant for the chrono-biostratigraphic  
713 correlations among sites at regional and continental scales (Müllenders et al., 1996; Tzedakis et al.,  
714 2001; Pini et al., 2009, 2010; Monegato et al., 2010).

715 The pollen records of GER1 and CB cores testify to alternating phases of cool to warm temperate  
716 forest and open vegetation, including xerophytic shrubs and steppe communities (Figs. 3, 4). These  
717 changes are mostly related to the Middle and Late Pleistocene glacial-interglacial cycles (Lisiecki



718 and Raymo, 2007; Wagner et al., 2019). Since both successions are mainly represented by fluvial  
719 deposits with proximal marine intercalations, percentage changes may be referred to either vegetation  
720 or pollen source changes and variations of pollen deposition/preservation potential, depending on,  
721 e.g., variations in the fluvial/tidal regime and depositional/taphonomical processes. Unfortunately,  
722 wide portions of both successions resulted barren in pollen content and, thus, our pollen records are  
723 not continuous. However, long chronological discontinuities within the sedimentary succession can  
724 be excluded because of the long-lasting subsidence of the Venetian plain (Massari et al., 2004;  
725 Barbieri et al., 2007).

726 The chrono-biostratigraphic correlation between the GER1 and CB cores - and their integration with  
727 global marine records (Lisiecki and Raymo, 2005) and alpine chronostratigraphy (Chaline and Jerz,  
728 1984) - are possible only merging all available multiproxy information (Figs. 5, 6). Applying such  
729 integrated approach, three main chronological and stratigraphic constrains were recognized (Figs. 2,  
730 5):

731 i) the first constrain is provided by the LGM aggradation phase. The great fluvial  
732 aggradation phase of the Brenta River megafan during this cold period (Iliceto et al., 2001;  
733 Mozzi, 2005; Mozzi et al., 2010; Ninfo et al., 2016; Rossato and Mozzi, 2016; Rossato et  
734 al., 2018) is well recognized in the sandy deposits of the stratigraphic units CB-VII, CB-  
735 VIII and GER1-VI. In CB core this sedimentation phase is constrained by two radiocarbon  
736 dates and its onset is marked by an erosional surface corresponding to the base of a fluvial  
737 channel. At the top of CB-VIII unit there is a well-developed soil (Soil 3-CB, Tab. 2), that  
738 was interpreted as the “caranto” paleosoil (Cucato et al., 2012; Mozzi et al., 2003; Mozzi  
739 et al., 2013). The thick sandy body recorded in GER1-VI unit is attributed to the LGM  
740 thanks to two radiocarbon dates. Here, the top of the succession (GER1-VII and GER1-  
741 VIII units) corresponds to the filling of the post-LGM incised valley of Padova (Cucato et  
742 al., 2012; Mozzi et al., 2013);

743 ii) the second constrain for the correlation between CB and GER1 core is a major paleosoil  
744 encountered in both cores (Soil 7-GER1, Soil 2-CB; Tab. 2). In CB core, this paleosoil  
745 lies within the uppermost relative warm phase, indicated by the pollen records of pollen  
746 zones CB8-CB12, and can be ascribed to the MIS 5. Instead, in GER1, it lies slightly  
747 below the uppermost relative warm phase, indicated by pollen zone GER1.7. Due to its  
748 stratigraphic positions, this sedimentary hiatus can be correlated with the erosional event  
749 observed in the Friulian plain (Pini et al., 2009; Monegato et al., 2010) and attributed to  
750 the MIS 5d glacioeustatic fall (Waelbroeck et al., 2002). Whilst in AzzanoX core this  
751 erosional surface cuts only part of the sediments associated to the pollen zones attributed  
752 to the Eemian Interglacial (Pini et al., 2009), in the Valeriano Creek succession the erosion  
753 was sufficiently strong to remove all the Eemian sediments (Monegato et al., 2010). The  
754 same erosional event is recorded also in the Lake Fimon, where the water level drop and  
755 the reduction of the lake surface occurred as a consequence of established dry conditions  
756 (Pini et al., 2010);

757 iii) the third main constrain for the correlation of GER1 and CB cores is the presence of a  
758 marine transgression corresponding to the base of penultimate warm (fully interglacial)  
759 phase recorded in both the cores (pollen zones GER1.3-GER1.5 and pollen zones CB2-  
760 CB5). The marine intercalations, attributed to open bay to lagoon conditions thanks to the  
761 micropaleontological content (biofacies A1 and A2) and the presence of marine mollusk  
762 shell fragments, are correlated through the lower part of GER1-III unit and CB-II unit.

763 The palynological results were entered in the correlation framework obtained from these three  
764 constrains, in order to reconstruct the climatostratigraphy of the two cores and to understand the  
765 environmental evolution of the Venetian plain since the Middle Pleistocene (Figs. 5, 6). For better  
766 clarity, we opted to discuss the meaning and correlation of the different palynological zones in the  
767 following paragraphs from the top down, i.e., in inverse stratigraphic order.

768

## 769 **5.1 The Last Glacial Maximum (LGM)**

770 The interpretation of the upper parts of the cores, chronologically well-framed thanks to radiocarbon  
771 dating, represents one of the correlation constrains described above. The palynological information  
772 confirm cold conditions ascribable to the LGM for comparison with other data in the area of Padova  
773 an in the whole Venetian plain (Müllenders et al., 1996; Miola et al., 2003, 2006; Mozzi et al., 2003).  
774 Indeed, the vegetation reconstructed in GER1.10 and CB14 zones is dominated by xerophytic herbs  
775 and shrubs with conifer grooves; this last persisted in the foreland also during the advanced stages of  
776 the LGM, as similarly showed for the Friulian plain (Monegato et al., 2007; Pini et al., 2009) and  
777 from the paleoclimatic simulations of Barron and Pollard (2002), which foresee a steep precipitation  
778 gradient across the Alps during MIS 3 and the LGM, allowing the survival of woody species on the  
779 southern side of the Alps.

780

## 781 **5.2 The Middle Würm and the identification of Early-Middle Würm boundary**

782 The palynological signal of the stadial phases of the Middle Würm is generally similar to the LGM  
783 one, and not always is easily distinguished from the interstadial phases features (Pini et al., 2009).  
784 The millennial-scale climatic oscillations characterizing MIS 3 and MIS 4 are only identified in high-  
785 resolution pollen records in Western and Southern Europe, where the sampling resolution is below  
786 300 yr (Allen et al., 2000; Tzedakis et al., 2004; Sánchez Goñi et al., 2008; Wohlfarth et al., 2008;  
787 Badino et al., 2019). Pollen zones GER1.8, GER1.9 and CB13 reflect open conifer-birch forest with  
788 abundant steppic and xerophytic communities and very rare temperate taxa, either reworked or  
789 referred to long-distance transport. The typical alternation between mixed conifer - *Betula* forest and  
790 expansion phases of steppic communities, recorded in the master cores of Venetian Friulian plain  
791 (AzzanoX and Fimon - Ponte sulla Debba cores), is unrecognizable here. However, these zones can  
792 be attributed to the Middle Würm (i.e., ca 35-75 ka) thanks to radiocarbon dating: in CB core a  
793 radiocarbon date allows to fix the base of LGM (Ua-24602 sample, Tab. 1), in GER1 core the sample  
794 ETH-74713 provides a radiocarbon age fully falling in the MIS 3.

795 Middle Würm is thus considered to include the upper parts of GER1-V and CB-VI stratigraphic units.  
796 The lower limit, currently set around 70 ka BP (Chaline and Jerz, 1984), is here based on the relative  
797 expansion of thermophilous trees recorded in CB12 pollen zone, whereas in GER1 core is assumed  
798 to correspond with the Soil 8-GER1, probably including the part of the second post-Eemian  
799 interstadial.

800 The modest thickness of the deposits associated to the MIS 3/4 is coherent with what observed in  
801 AzzanoX core (Pini et al., 2009) and in some other cores of the Friulian plain (CNC4, LUG, VV,  
802 PCN) where the lagoon deposits of the Tyrrhenian transgression are found few meters below the MIS  
803 3 deposits, suggesting the existence of a sedimentary gap which comprises large part of Middle Würm  
804 (Feruglio, 1936; Fontana et al., 2010a, 2010b).

805

### 806 **5.3 Identification of the Eemian Interglacial and vegetation changes during the stadial-** 807 **interstadial sequence in the Early Würm**

808 The deposits associated to the lower part of GER1-V (37.40-50.15 m of depth) and the upper part of  
809 GER1-IV (50.15-54.95 m of depth) stratigraphic units, as well the lower part of CB-VI (33.52-50.67  
810 m of depth) and the upper part of CB-V (50.67-52.55 m of depth) stratigraphic units, are embedded  
811 between the Middle Würm deposits and a deeper, pronounced cold phase (pollen zones GER1.6 and  
812 CB7). The vegetation successions of pollen zones GER1.7 and CB12-CB8, are the uppermost ones  
813 to present a more or less marked occurrence of temperate taxa.

814 In the circumalpine region, the Eemian Interglacial is characterized by high afforestation (AP>85%)  
815 with dominance of thermophilous and mesophilous trees and shrubs with abundant *Carpinus* and  
816 *Quercus* and low occurrence of *Fagus* (Woillard, 1978; Müllenders et al., 1996; Reille et al., 1998;  
817 Drescher-Schneider, 2000; Pini et al., 2009, 2010). The CB8 pollen zone reflects this condition and  
818 is topped by the paleosoil (Soil 2-CB, Tab. 2) related to the glacioeustatic sea-level drop coincident  
819 with MIS 5d and described as one of our three correlation constrains. GER1 core does not present a  
820 pollen zone with similar vegetation assemblage, however, two sterile levels (54.56 m, 52.02 m of

821 depth) occurs immediately below the paleosoil (Soil 7-GER1) correlated with Soil 2-CB. Likely, the  
822 pedogenetic processes of oxidation may have deteriorated the pollen content, determining the absence  
823 of pollen within the deposits associated to the last interglacial. Above this stratigraphic unconformity,  
824 an alternation between arboreal cool and warm phases is recorded, more pronounced in CB core,  
825 probably due to the higher sampling frequency. Conditions of persistent afforestation, with changes  
826 in forest composition and phases with slightly minor opening of forest canopy are coherent with what  
827 recorded in the Early Würm of the Venetian plain (Pini et al., 2010), and may reflect the post-Eemian  
828 stadial-interstadial sequence.

829

830 In CB core, the pollen zone CB9 seems to represent a *Pinus-Picea* open forest that can be associated  
831 to the first stadial occurred after the Eemian Interglacial, whereas the CB10 pollen zone indicates a  
832 new phase of mixed forest dominated by warm-temperate broad-leaved trees and characterized by  
833 the expansion of *Fagus*. Since the occurrence of *Fagus* allows to distinguish post-Eemian interstadial  
834 from the last Interglacial (Tzedakis et al, 2001; Magri et al., 2006; Pini et al., 2009, 2010), CB10  
835 pollen zone is attributed to the first post-Eemian interstadial (related to MIS 5c). *Carpinus*, abundant  
836 during the Eemian, is still a main forest tree, whereas *Abies* is present with low percentage. Based on  
837 the stratigraphic position and the similar pollen assemblage, we correlate GER1.7 pollen zone to the  
838 same interstadial. The forest canopy experienced an opening reduction in CB11 pollen zone, which  
839 is characterized by *Pinus* dominance with xerophytic elements. The almost total absence of warm-  
840 temperate taxa suggests a relatively cold and dry phase ascribable to the second post-Eemian stadial  
841 (related to MIS 5b), not identified in GER1 core, during which one of the most extreme trees  
842 population crashes is assumed (Tzedakis et al., 2003).

843 A controversial point is the punctual presence of halophytes within CB11 zone, which is unlikely  
844 related to salt marshes or microtidal flooding processes since, according to Antonioli et al. (2004), at  
845 global scale, the sea level dropped at about -60 m below the present position during MIS 5d, rising to  
846 -20 m during the subsequent interstadials (MIS 5c and MIS 5a). Moreover, the micropaleontological

847 data, although not abundant, indicate a continental environment. Broad-leaved temperate forest  
848 expands again in pollen zone CB12 but not as extensively as during the Eemian and the first post-  
849 Eemian interstadial, coherently with the vegetation association observed during the second post-  
850 Eemian interstadial in AzzanoX and Lake Fimon records (Pini et al., 2009, 2010). In GER1 core MIS  
851 5a is not supported by palynological data, probably due to the pedogenic processes associated to Soil  
852 8-GER1 development.

853 The Early Würm misses here the continuative abundance of *Picea*, recorded in the circumalpine  
854 records (Pini et al., 2009).

855

#### 856 **5.4 Vegetation and fluvio-glacial aggradation evidence during the penultimate glaciation**

857 Between 54.95 and 72.35 m of depth, GER1 core presents a prevalently medium-coarse fluvial sand  
858 unit characterized by the presence of organic and peaty intercalations (stratigraphic unit GER1-IV).  
859 The lithofacies suggest similarities with the glaciofluvial aggradation phase occurred during the  
860 LGM, an interpretation supported also by the few available palynological information in the upper  
861 part of the stratigraphic unit, which indicate cold and dry continental climatic conditions (pollen zone  
862 GER1.6).

863 Similar features are recorded in the upper part of CB-IV stratigraphic unit, which also shows the  
864 establishment of a sandy channel body, and CB7 pollen zone, reflecting a *Pinus* forest with scattered  
865 *Picea* and xerophytic shrubs.

866 This alluvial interval is constrained at the top by the Eemian forest succession in CB core and by the  
867 deposits ascribed to MIS 5e in GER1 core. Below, there are the thick stratigraphic units GER1-III  
868 and CB-II, characterized at the bottom by the marine intercalation that constitutes our third main  
869 correlation constrain.

870 These considerations support the attribution of this interval to the penultimate glaciation (54.95-72.35  
871 m of depth in GER1 core and 52.55-67.70 m in CB core), during which the full glacial conditions led  
872 to high sediment yield from the outwash streams, fed by the Alpine glaciers reaching the frontal

873 position in the piedmont area (Venzo, 1977; Carton et al., 2009; Rossato et al., 2013). In this context  
874 the Venetian-Friulian plain aggraded up to 20-30 m (Fontana et al., 2010a).

875 Whilst in GER1 core the beginning of the penultimate glaciation is fixed in coincidence with the  
876 abrupt transition to prevalently sandy fluvial aggradation (72.35 m of depth), in CB it is identified by  
877 the pollen assemblage of zone CB6. Indeed, it shows an interstadial signature with persistent  
878 temperate taxa in low percentage, likely framed within the millennial climatic oscillations occurred  
879 during the early MIS 6, before the extreme cooling (pollen zone CB7) coinciding with the beginning  
880 of the penultimate glacial maximum (i.e. about 150 ka; Martrat et al., 2004).

881

## 882 **5.5 Evidence of a sea level highstand and identification of MIS 7**

883 The depositional, macro- and micropaleontological data of GER1-III and CB-II stratigraphic units  
884 (biofacies A1 and A2), highlights the presence of a paralic environment, probably recording a  
885 transgression-regression cycle, although a clear ravinement surface is not identified. These deposits  
886 are characterized by a pollen content typical of a temperate climate in both the cores (GER1.3-5 and  
887 CB2-5 pollen zones). Assuming prevalently continuous sedimentation, we refer this interval to MIS  
888 7, as it is overlaid in both the cores by a pronounced cold phase (pollen zones GER1.6 and CB7)  
889 followed by the Eemian Interglacial (pollen zone CB8). This interpretation is consistent with the  
890 AzzanoX core succession, in which a clear bathymetric curve for MIS 7 is reconstructed, whereas  
891 continuous continental conditions are observed throughout the last interglacial (Pini et al., 2007,  
892 2009). Although the co-dominance *Abies-Fagus*, diagnostic of the late MIS 7, is not recorded neither  
893 in GER1 nor in CB cores, the association of *Fagus* with frequent *Carpinus betulus* supports the  
894 attribution to the MIS 7 (Tzedakis et al., 2001). Whilst in GER1 core the pollen samples frequency is  
895 too low for identifying the stadial-interstadial succession visible in pollen records attributed to MIS  
896 7, in CB core the samples are enough to hypothesize a climatic sequence. In particular, the open  
897 vegetation reflected by the pollen zone CB4 is consistent with a stadial phase, likely framed as  
898 substage b. Indeed, according to Tzedakis et al. (2003) the persistence of significant tree population

899 is recorded in Mediterranean records, in accordance with continuous moisture availability during this  
900 period, contrary to what observed during substage 7d (Reille and de Beaulieu, 1995; Reille et al.,  
901 1998). The stadial interval thus identified, is embedded between two temperate phases (pollen zones  
902 CB2-3 and CB5). Pollen zone CB3 shows the largest and floristically diverse forest expansion of MIS  
903 7 interval, with thermophilous elements abundance values among the highest in the whole core. A  
904 similar situation is observed during substage c in Valle di Castiglione and Tenaghi Philippon pollen  
905 records (Van der Wiel and Wijstra, 1987; Follieri et al., 1988; Tzedakis et al., 2003). Pollen zone  
906 CB2 shows low AP sum; however, it presents a clear *Carpinus betulus* dominance, attributable to  
907 MIS 7c according to Tzedakis et al. (2001), and is associated with the paralic deposits of stratigraphic  
908 unit CB-II and separated from the upper zone by a 13.08 m-thick interval of shore-face sand. The  
909 amplitude of sea-level changes during MIS 7 is still poorly understood (Bard et al., 2002), however  
910 according to Dutton et al. (2009), the MIS 7.3 highstand was lower than the MIS 7.5 and MIS 7.1  
911 highstands at Argentarola Cave (central Italy). Nevertheless, the lack of major unconformities, the  
912 strong interstadial signature of pollen zones CB2-3 and the evident absence of a pronounced cold and  
913 dry phase attributable to substage d, allows to hypothesize the correspondence of pollen zones CB2-  
914 3 to MIS 7c and CB5 to MIS 7a.

915

## 916 **5.6 Pre-MIS 7/8 continental deposits**

917 GER1 and CB cores have a depth difference of 15.65 m, which prevents the chrono-biostratigraphic  
918 correlation of the GER1 basal units.

919 Below the MIS 7 proximal marine deposits, CB core shows a 3.77 m-thick basal unit constituted by  
920 alluvial sediments (CB-I stratigraphic unit) characterized by pollen originating from a pine forest  
921 (CB1 pollen zone). Despite the presumed stratigraphic continuity, the attribution of this interval to  
922 the early MIS 7 is excluded, as the pollen signature of the unique sample does not reflect neither the  
923 extremely dry and cold vegetation of the substage 7d, nor the substage 7e warm phase (Follieri et al.,  
924 1988; Reille et al., 1998; Tzedakis et al., 1997, 2001, 2003). A clear attribution to the marine isotopic



925 stage is difficult, however MIS 8 may be supposed. The limited thickness of the fluvial deposits  
926 attributed to MIS 8 is coherent with the limited extent of this glaciation in Europe in respect to MIS  
927 6 (Batchelor et al., 2019).

928 A similar pollen zone is not observed in GER1 core, where a 11.11 m-thick alluvial interval barren  
929 in pollen separate the MIS 7 paralic deposits from an important organic level rich in pollen. This last  
930 shows a mixed temperate forest (pollen zone GER1.1) evolving to a conifer-dominated one (pollen  
931 zone GER1.2), not interpretable as MIS 8 because of the abundance of broad-leaved trees, hence  
932 older than this stage. Referring to the Central-European records (e.g, Reille and de Beaulieu, 1995;  
933 Reille et al., 1998), coherently with what was done for AzzanoX core (Zanferrari et al., 2008), the  
934 continuous presence of *Pterocarya* in the lower zone GER1.1, recalls the MIS 11 interstadials.  
935 Nevertheless, we should consider the complex stratigraphic distribution of this taxon in the  
936 Mediterranean area (Tzedakis et al., 2001), where it makes the last appearance in MIS 11c in southeast  
937 Greece (Okuda et al., 2001), whereas it persists during MIS 9e at Tenaghi Philippon (Van der Wiel  
938 and Wijstra, 1987) and throughout MIS 7 at Valle di Castiglione (Follieri et al., 1988). Moreover, the  
939 great *Abies* expansion observed during the Holstein/Praclaux Interglacial in all the available records  
940 (Tzedakis et. al, 2001; Zanferrari et al., 2008) misses in GER1 core, whereas the supposed presence  
941 of two species of *Abies* (i.e., *Abies* and *Abies* cfr. based on morphological and morphometrical  
942 features) is observed in pollen zones GER1.1, GER1.2, GER1.3. up to GER1.5.

943 On the other hand, according to Tzedakis et al. (2003), MIS 11 shows two peaks of temperate taxa  
944 (MIS 11a, c) and a *Pinus* dominated substage (MIS 11b), which may recall GER1.2 pollen zone.

945 The ambiguity in chronologically framing the upper peak of *Pterocarya* is observed also in the nearby  
946 and deeply studied Venezia1 core (Müllenders et al., 1996; Kent et al., 2002; Massari et al., 2004),  
947 where it occurs in correspondence of a transgressive surface at 262 m of depth. In this core, the  
948 available magnetostratigraphic and biostratigraphic constrains allow to relate sapropel VS02 to the  
949 Sb, to assign it an age of 0.597 Ma (Langereis et al., 1997) and to fix the Eemian transgression at 79  
950 m of depth. Kent et al. (2002) proposed two alternative age models for the section of the Venezia1

951 core above 572.4 m. The first model, justified by a linear subsidence rate of 180 m/Ma, considers the  
952 transgression with the last occurrence of *Pterocarya* coincident with the transition between MIS 12  
953 and MIS 11. Consequently, in the Venezia1 core the transition between MIS 8 and MIS 7 corresponds  
954 with a transgression surface at 152 m of depth, about 50 m deeper than in GER1 and CB core;  
955 moreover, the Venezia1 core record assumes that *Pterocarya* disappeared in the Venetian plain after  
956 MIS 11.

957 Age Model 2 assumes that the stratigraphically-highest occurrence of *Pseudoemiliana lacunosa* at  
958 562.4 m corresponds with its last appearance datum, an event considered to be globally synchronous  
959 and associated with the upper part of MIS 12 (Thierstein et al., 1977). According to this model,  
960 supported by an irregular subsidence pattern with an average rate of 360 m/Ma, the transgressive  
961 surface rich in *Pterocarya* corresponds with the transition between MIS 8 and MIS 7 which is thus  
962 located about 160 m below the GER1 and CB one. Moreover, according to this age model, *Pterocarya*  
963 persisted in the Venetian plain even after MIS 11.

964 Assuming the validity of one or the other model for the Venice area significantly changes the  
965 interpretation of the pollen zones GER1.1 and GER1.2. Age Model 1 allows to assume that the  
966 occurrence of *Pterocarya* in GER1 core is coincident or older to its last appearance during MIS 11 in  
967 the Venetian plain. This interpretation is justified assuming large sedimentary gaps in the depth  
968 interval where 5 paleosoils are observed in unit GER1-II. On the other hand, our observations suggest  
969 that these paleosoils are poorly developed (Tab. 2) and unlikely represent large gaps, inducing to  
970 consider a stratigraphic continuity and to adopt the Age Model 2. Since according to this model,  
971 *Pterocarya* is present after MIS 11, pollen zones GER1.1 and GER1.2 would coincide with MIS 9.  
972 Nevertheless, the consequent depth difference between the first MIS 7 surface transgression in  
973 Venezia1 and the MIS 7.3 one in GER1-CB cores (about 160 m) seems to be too significant.  
974 The discussion therefore remains open, since the only palynological data available is insufficient to  
975 certainty frame this interval and the closer deep information from the Venezia1 core are still debated  
976 (Kent et al., 2002; Massari et al., 2004).

977 The gravelly basal portion of GER1 (stratigraphic unit GER1-I) misses palynological and  
978 micropaleontological information. The unique stratigraphic data seems to refer these deposits to the  
979 infilling of a fluvial incised channel, established within the alluvial plain during a deglaciation erosive  
980 phase related to a glacial interval older than MIS 8.

981

## 982 **6. Conclusions**

983 The sedimentary successions of GER1 and CB cores provide a new, continuous archive of the long-  
984 term sedimentary, climatic and environmental evolution of the south-eastern Alpine foreland,  
985 allowing to investigate the Middle-Upper Pleistocene and to reconstruct the climate history of the  
986 Central Venetian plain since MIS 7. Palynological analysis in GER1 brings new data on the debate  
987 on the pre-Eemian evolution of the Venetian plain (e.g., Kent et al., 2002; Massari et al., 2004) and  
988 the chronology of the last occurrence of *Pterocarya* in the southern alpine area, as this core yielded a  
989 deep stratigraphic interval rich in this taxon and older than MIS 8, not yet definitively interpreted as  
990 for its chronology.

991 The stratigraphic and paleontological analyses show that both cores mainly cross alluvial deposits,  
992 with evidence of one proximal marine intercalation. Unconventionally, the palynostratigraphic  
993 method was applied to both core successions, which were simultaneously interpreted due to their  
994 proximity, merging all available multiproxy information in order to reconstruct the climatic and  
995 stratigraphic evolution of the basin.

996 Despite the presence of paleosoils, erosional surfaces and levels barren in pollen, an overall  
997 stratigraphic continuity was recognized in the successions. The joint interpretation of the two cores  
998 allowed to design a robust chronological model that comprises the last two glaciations (i.e., MIS 6  
999 and 2).

1000 The palynological data allow to link the stratigraphic units to major climatic fluctuations, indicating  
1001 the unique transgression interval as the interglacial MIS 7.3 (i.e about 220-210 ka BP), and to  
1002 highlight the continuous continental conditions of the area of Padova during the Last Interglacial, in

1003 agreement with what observed in the Friulian Plain (Pini et al., 2009). The robust stratigraphic  
1004 correlation between GER1 and CB cores and the correlation with the reference records in the  
1005 Venetian-Friulian plain (Zanferrari et al., 2008; Pini et al., 2009, 2010; Monegato et al., 2010, 2011),  
1006 allow to identify the Eemian level in the composite section, even if GER1 core lacks the related  
1007 palynological information. The stratigraphic positions of the stadials and interstadials phases were  
1008 also outlined basing on the integration of lithostratigraphic and palynostratigraphy information.  
1009 The palynological constrains allow to chronologically frame two important phases of glaciofluvial  
1010 aggradation, correlating them to the last two glacial culminations. The penultimate glacial  
1011 culmination (i.e. late MIS 6, about 148-135 ka BP) is embedded between the late MIS 7 and the  
1012 Eemian deposits, whereas the LGM (i.e. 26.5-19 ka cal BP) follows the Eemian deposition and is  
1013 further constrained by radiocarbon dating. The Middle Würm is underrepresented with no evidence  
1014 for a glacial acme during MIS 4.  
1015 The occurrence of hiatuses and levels poor in pollen deeper than the MIS 8 deposits in GER1 prevents  
1016 the certain attribution of the lower two pollen zones to either MIS 11 or MIS 9. This question, still  
1017 unsolved, would require further studies on others pollen-rich, deeper successions, not yet available in  
1018 the area.

1019

## 1020 **Acknowledgements**

1021 This research did not receive any specific grant from funding agencies in the public, commercial, or  
1022 not-for-profit sectors. During its development A.M. benefited from a PhD scholarship of the  
1023 University of Padova. The authors wish to thank Maurizio Cucato and Gianna Valentini for their  
1024 contribution to the stratigraphic and palynological analysis of CB core, within the Italian National  
1025 Project of Geological Cartography at scale 1:50,000 (CARG Project), sheet Padova Sud.  
1026 Moreover, we are grateful to Antonio Galgaro and Giorgia Dalla Santa (University of Padova) for  
1027 having allowed access to the GER1 core.

1028

1029 **References**

1030 Accordi, B., 1950. Esame geologico-paleontologico di un pozzo terebrato a Cartura (Padova). Mem.  
1031 Ist. Geol. Univ. Padova, 16, 1-19.

1032

1033 Allen, J.R.M., Watts, W.A., Huntley, B., 2000. Weichselian palynostratigraphy, palaeovegetation and  
1034 palaeoenvironments; the record from Lago Grande di Monticchio, southern Italy. *Quatern. Int.* 73/74,  
1035 91-110.

1036

1037 Antonioli, F., Bard, E., Silenzi, S., Potter, E.K., Improta, S., 2004. 215-kyr history of sea level based  
1038 on submerged speleothems. *Global Planet. Change* 43, 57-68.

1039

1040 Avanzini, M., Bargossi, G.M., Borsato, A., Selli, L., 2010. Note Illustrative della Carta Geologica  
1041 d'Italia alla scala 1: 50.000, Foglio 060- Trento, ISPRA-Servizio Geologico d'Italia, Trento.

1042

1043 Badino, F., Pini, R., Ravazzi, C., Margaritora, D., Arrighia, S., Bortolinia, E., Figusa, C., Biagio  
1044 Giaccio, B., Luglia, F., Marciana, G., Monegato, G., Moronic, A., Negrino, F., Oxilia, G., Peresani,  
1045 M., Romandini, M., Ronchitelli, A., Spinapolice, E.E., Zerboni, A., Benazzi, S., 2019. An overview  
1046 of Alpine and Mediterranean palaeogeography, terrestrial ecosystems and climate history during MIS  
1047 3 with focus on the Middle to Upper Palaeolithic transition. *Quatern. Int.*, ISSN 1040-6182.  
1048 <https://doi.org/10.1016/j.quaint.2019.09.024>.

1049

1050 Barbieri, C., Di Giulio, A., Massari, F., Asioli, A., Bonato, M., Mancin, N., 2007. Natural subsidence  
1051 of Venice area during the last 60 My. *Basin Res.* 19/1, 105-123.

1052

1053 Bard, E., Antonioli, F., Silenzi, S., 2002. Sea-level during the penultimate interglacial period based  
1054 on submerged stalagmite from Argentarola Cave (Italy). *Earth Plan. Sci. Lett.* 196 (3-4), 135-146.

1055

1056 Barron, E., Pollard, D., 2002. High-resolution climate simulations of Oxygen Isotope Stage 3 in  
1057 Europe. *Quaternary Res.* 58, 296-309.

1058

1059 Batchelor, C.L., Margold, M., Krapp, M., Murton, K.D., Dalton, A.S., Gibbard, P.L., Stockes, C.R.,  
1060 Murton, J.B., Manica, A., 2019. The configuration of Northern Hemisphere ice sheets through the  
1061 Quaternary. *Nat. Commun.* 10, 3713, <https://doi.org/10.1038/s41467-019-11601-2>.

1062

1063 Berglund, B.E., 1986. *Handbook of Holocene palaeoecology and palaeohydrology*. Wiley-  
1064 Interscience; John Wiley & Sons Ltd., Chichester. *J. Quaternary Sci.*, 1: 86-87.  
1065 doi:10.1002/jqs.3390010111.

1066

1067 Beug, H.J., 2004. *Leitfaden der Pollenbestimmung für Mitteleuropa und angrenzende Gebiete*. Verlag  
1068 Dr. Friedrich Pfeil, München.

1069

1070 Bortolami, G.L., Carbognin, L., Gatto, P., 1984. The natural subsidence in the Lagoon of Venice,  
1071 Italy. *Land Subsidence, IAHS Publications 151*, 777-785.

1072

1073 Braconnot, P., Otto-Bliesner, B., Harrison, S., Joussaume, S., Peterchmitt, J.-Y., Abe-Ouchi, A.,  
1074 Crucifix, M., Driesschaert, E., Fichefet, Th., Hewitt, C.D., Kageyama, M., Kitoh, A., Laîné, A.,  
1075 Loutre, M.-F., Marti, O., Merkel, U., Ramstein, G., Valdes, P., Weber, S.L., Yu, Y., Zhao, Y., 2007.  
1076 Results of PMIP2 coupled simulations of the Mid-Holocene and Last Glacial Maximum – Part 1:  
1077 experiments and large-scale features, *Clim. Past* 3, 261-277, <https://doi.org/10.5194/cp-3-261-2007>.

1078

1079 Bronk Ramsey, C., 2009. Bayesian analysis of radiocarbon dates. *Radiocarbon* 51(1), 337-360.

1080

1081 Carbognin, L., Tosi, L., 2002. Interaction between climate changes, eustasy and land subsidence in  
1082 the North Adriatic Region, Italy. *Marine Ecology* 23 (Suppl. 1), 38-50.

1083

1084 Carton, A., Bondesan, A., Fontana, A., Meneghel, M., Miola, A., Mozzi, P., Primon, S., Surian, N.,  
1085 2009. Geomorphological evolution and sediment transfer in the Piave River watershed (north-eastern  
1086 Italy) since the LGM. *Géomorphologie: relief, Processus. Environment* 3, 37-58.

1087

1088 Castiglioni, G.B., 1999. Geomorphology of the Po Plain. *Geogr. Fis. Din. Quat.* (Suppl. 3), 7-20.

1089

1090 Chaline, J., Jerz, H., 1984. Arbeitsergebnisse der Subkommission für Europäische Quartärstratigraphie:  
1091 Stratotypen des Würm-Glazials (Bericht SEQS 5). *Eiszeitalter und Gegenwart* 34, 185-206.

1092

1093 Clark, P., Dyke, A., Shakun, J., Carlson, A., Clark, J., Wohlfarth, B., Mitrovica, J., Hostetler, S.,  
1094 McCabe, A., 2009. The Last Glacial Maximum. *Science* 325, 710-714,

1095

1096 Cucato, M., De Vecchi, G.P., Mozzi, P., Abbà, T., Paiero, R., Sedeà, R. (Eds.), 2012. Note Illustrative  
1097 della Carta geologica d'Italia alla scala 1:50.000, Foglio 147 Padova Sud. ISPRA-Servizio Geologico  
1098 d'Italia – Regione Veneto. LTS Land Technology & Services, Padova e Treviso.

1099

1100 Dieni, I., Proto Decima, F., 1960. Studio paleontologico - stratigrafico di un pozzo perforato nell'orto  
1101 Botanico dell'Università di Padova: Memorie Acc. Patavina di SS. LL. AA; Classe di SC. Mat. e Nat.  
1102 73, 3-16.

1103

1104 Drescher-Schneider, R., 2000. The Riss-Würm interglacial from West to East in the Alps: an  
1105 overview of the vegetational succession and climatic development. *Geologie en Mijnbouw.*  
1106 *Netherlands Journal of Geosciences* 79 (2/3), 233-239, doi: 10.1017/S0016774600023672.

1107

1108 Duprat- Oualid, F., Rius, D., Bégeot, C., Magny, M., Millet, L., Wulf, S., Appelt, O., 2017.  
1109 Vegetation response to abrupt climate changes in Western Europe from 45 to 14.7k cal a BP: the  
1110 Bergsee lacustrine record (Black Forest, Germany). *J. Quaternary Sci.*, 32: 1008-1021.  
1111 <https://doi.org/10.1002/jqs.2972>.

1112

1113 Dutton, A., Bard, E., Antonioli, F., Esat, M.T., 2009. Phasing and amplitude of sea-level and climate  
1114 change during the penultimate interglacial. *Nature Geoscience* 2, 355-359  
1115 <https://doi.org/10.1038/ngeo470>.

1116

1117 Fægri, K., Iversen, J., 1989. Textbook of pollen analysis. 4th ed. by K. Fægri, P.E. Kaland & K.  
1118 Krzywinski. John Wiley & Sons, Chichester.

1119

1120 Feruglio, E., 1936. Sedimenti marini nel sottosuolo della bassa pianura friulana. *Boll. Soc. Geol. It.*  
1121 55(1), 129-138.

1122

1123 Follieri, M., Magri, D., Sadori, L., 1988. 250,000-year pollen record from Valle di Castiglione  
1124 (Roma). *Pollen Spores* 30, 329-356.

1125

1126 Fontana, A., Mozzi, P., Bondesan, A., 2008. Alluvial megafans in the Venetian - Friulian Plain (north-  
1127 eastern Italy): evidence of sedimentary and erosive phases during Late Pleistocene and Holocene.  
1128 *Quatern. Int.* 189, 71-90.

1129

1130 Fontana, A., Mozzi, P., Bondesan, A., 2010a. Late Pleistocene evolution of the Venetian - Friulian  
1131 Plain. *Rendiconti Lincei Scienze Fisiche e Naturali* 21, Supp. 1, 181-196.

1132



1133 Fontana, A., Bondesan, A., Meneghel, M., Toffoletto, F., Vitturi, A., Bassan, V., 2010b. Note  
1134 illustrative della Carta Geologica d'Italia alla scala 1:50.000. Foglio 107, Portogruaro. ISPRA-  
1135 Regione del Veneto, Roma.

1136

1137 Fontana, A., Mozzi, P., Marchetti, M., 2014. Alluvial fans and megafans along the southern side of  
1138 the Alps. *Sediment. Geol.* 301, 150-171.

1139

1140 Garzanti, E., Vezzoli, G., Andò, S., 2011. Paleogeographic and paleodrainage changes during  
1141 Pleistocene glaciations (Po Plain, Northern Italy). *Earth Science Rev.* 105(1-2), 25-48. doi:  
1142 [10.1016/j.earscirev.2010.11.004](https://doi.org/10.1016/j.earscirev.2010.11.004).

1143

1144 Grimm, E., 1991-2019. Tilia, Version 2.6.1 Illinois State Museum, Research and Collection Center,  
1145 Springfield.

1146

1147 Gröger, E., 1989. Palynostratigraphy of the last interglacial/glacial cycle in Germany. *Quatern. Int.*  
1148 3/4, 69-79.

1149

1150 Heiri, O., Koinig, K. A., Spötl, C., Barrett, S., Brauer, A., Drescher-Schneider, R., Gaar, D., Ivy-  
1151 Ochs, S., Kerschner, H., Luetscher, M., Moran, A., Nicolussi, K., Preusser, F., Schmidt, R.,  
1152 Schoeneich, P., Schwörer, C., Sprafke, T., Terhorst, B., Tinner, W., 2014. Palaeoclimate records 60-  
1153 8 ka in the Austrian and Swiss Alps and their forelands. *Quaternary Sci. Rev.* 106, 186-205.  
1154 <https://doi.org/10.1016/j.quascirev.2014.05.021>.

1155

1156 Huntley, B. & Birks, H. J. B. 1983. An atlas of past and present pollen maps for Europe: 0-13,000  
1157 years ago. Cambridge: University Press. *Antiquity*, 58(223), 154-155.  
1158 doi:10.1017/S0003598X00051814.

1159

1160 Iliceto, V., Meloni, F., Mozzi, P., Rizzetto, F., 2001. Il sottosuolo della Cappella degli Scrovegni a  
1161 Padova. *Geol. Tec. Ambient.* 9, 3-17.

1162

1163 Jahn, R., Blume, H.P., Asio, V.B., Spaargaren, O., Schad, P., Langohr, R., Brinkman, R.,  
1164 Nachtergaele, F.O., Pavel Krasilnikov, R., 2006. *Guidelines for Soil Description*. FAO, Rome, p. 97.

1165

1166 Jorissen, F.J., 1987. The distribution of benthic foraminifera in the Adriatic Sea. *Mar.*  
1167 *Micropalaeontol.* 12(1), 21-48.

1168

1169 Kent, D.V., Rio, D., Massari, F., Kukla, G., Lanci, L., 2002. Emergence of Venice during the  
1170 Pleistocene. *Quaternary Sci. Rev.* 21, 1719-1727.

1171

1172 Lisiecki, L.E., Raymo, M.E., 2005. A Pliocene-Pleistocene stack of 57 globally distributed benthic  
1173  $\delta^{18}\text{O}$  records. *Paleoceanography* 20, PA1003, doi: 10.1029/2004PA001071.

1174

1175 Lisiecki, L.E., Raymo, M.E., 2007. Plio-Pleistocene climate evolution: trends and transitions in  
1176 glacial cycle dynamics. *Quaternary Sci. Rev.* 26, 1-2, 56-69.  
1177 <https://doi.org/10.1016/j.quascirev.2006.09.005>.

1178

1179 Löffverström, M., 2020. A dynamic link between high-intensity precipitation events in southwestern  
1180 North America and Europe at the Last Glacial Maximum. *Earth Planet. Sci. Lett.* 534, 116081.

1181

1182 Löffverström, M., Caballero, R., Nilsson, J., Kleman, J., 2014. Evolution of the large-scale  
1183 atmospheric circulation in response to changing ice sheets over the last glacial cycle. *Clim. Past* 10,  
1184 1453-1471. doi:10.5194/cp-10-1453-2014.

1185

1186 Luetscher, M., Boch, R., Sodemann, H., Spötl, C., Cheng, H., Edwards, R.L., Frisia, S., Hof, F.,  
1187 Müller, W., 2005. North Atlantic storm track changes during the Last Glacial Maximum recorded by  
1188 Alpine speleothems. *Nat. Commun.* 6, 6344. doi: 10.1038/ncomms7344.

1189

1190 Magri, D., Vendramin, G.G., Comps, B., Dupanloup, I., Geburek, T., Gömöry, D., Latalowa, M., Litt,  
1191 T., Paule, L., Roure, J.M., Tantau, I., van der Knaap, W.O., Petit, R.J., Beaulieu, J.-L. de, 2006. A  
1192 new scenario for the Quaternary history of European beech populations: palaeobotanical evidences  
1193 and genetic consequences. *New Phytologist* 171, 199-221.

1194

1195 Mancin, N., Di Giulio, A., Cobianchi, M., 2009. Tectonic vs. climate forcing in the Cenozoic  
1196 sedimentary evolution of a foreland basin (Eastern Southalpine system, Italy). *Bas. Res.* 21(6), 799-  
1197 823. doi: 10.1111/j.1365-2117.2009.00402.

1198

1199 Martinson, D.G., Pisias, N.G., Hays, J.D., Imbrie, J., Moore, T.C., Shackleton, N.J., 1987. Age dating  
1200 and the orbital theory of the ice ages: development of a high-resolution 0 to 300,000-year  
1201 chronostratigraphy. *Quaternary Res.* 27,1-29.

1202

1203 Martrat, B., Grimalt, J.O., Lopez-Martinez, C., Cacho, I., Sierro, F.J., Flores, J.A., Zahn, R., Canals,  
1204 M., Curtis, J.H., Hodell, D.A., 2004. Abrupt temperature changes in the western Mediterranean over  
1205 the past 250,000 years. *Science* 306, 1762-1765.

1206

1207 Massari, F., Grandesso, P., Stefani, C., Jobstraibizer, P.G., 1986. A small polyhistory foreland basin  
1208 evolving in a context of oblique convergence: the Venetian basin (Chattian to Recent, Southern Alps,  
1209 Italy). in: Allen, P.A., Homewood, P. (Eds.), *Foreland Basins*. Blackwell Publishing Ltd, Oxford,  
1210 United Kingdom. doi:10.1002/9781444303810.ch7.

1211

1212 Massari, F., Rio, D., Serandrei Barbero, R., Asioli, A., Capraro, L., Fornaciari, E., Vergerio, P.P.,  
1213 2004. The environment of Venice area in the past two million years. *Palaeogeogr. Palaeoclimatol.*  
1214 *Palaeoecol.* 202, 273-308.

1215

1216 Miola, A., Albanese, D., Valentini, G., Corain, L., 2003. Pollen data for a biostratigraphy of LGM in  
1217 the Venetian Po Plain. *Il Quaternario* 16, 21-26.

1218

1219 Miola, A., Bondesan, A., Corain, L., Favaretto, S., Mozzi, P., Piovan, S., Sostizzo, I., 2006. Wetlands  
1220 in the Venetian Po Plain (north-eastern Italy) during the Last Glacial Maximum: vegetation,  
1221 hydrology, sedimentary environments. *Rev. Palaeobot. Palyno.* 141(1), 53-81.

1222

1223 Miola, A., 2012. Tools for Non-Pollen Palynomorphs (NPPs) analysis: A list of Quaternary NPP  
1224 types and reference literature in English language (1972–2011). *Rev. Palaeobot. Palyno.*, 186, 142-  
1225 16.

1226

1227 Monegato, G., Ravazzi, C., Donegana, M., Pini, R., 2007. Evidence of a two-fold glacial advance  
1228 during the Last Glacial Maximum in the Tagliamento end moraine system (eastern Alps). *Quaternary*  
1229 *Res.* 68, 284-302.

1230

1231 Monegato, G., Lowick, S.E., Ravazzi, C., Banino R., Donegana, M., Preusser, F., 2010. Middle to  
1232 Late Pleistocene chronology and palaeoenvironmental evolution of the south-eastern Alpine  
1233 Foreland: the Valeriano Creek succession (NE Italy). *J. Quaternary Sci.* 25, 617-632.

1234

1235 Monegato, G., Pini, R., Ravazzi, C., Reimer, P. J., Wick, L., 2011. Correlating Alpine glaciation with  
1236 Adriatic sea-level changes through lake and alluvial stratigraphy, *J. Quaternary Sci.* 26, 791-804.  
1237 <https://doi.org/10.1002/jqs.1502>.  
1238  
1239 Monegato, G., Ravazzi, C., Culiberg, M., Pini, R., Miloš, B., Calderoni, G., Jež, J., Perego, R., 2015.  
1240 Sedimentary evolution and persistence of open forests between the south-eastern Alpine fringe and  
1241 the Northern Dinarides during the Last Glacial Maximum. *Palaeogeogr. Palaeoclimatol. Palaeoecol.*  
1242 436. 23-40.  
1243  
1244 Monegato, G., Scardia, G., Hajdas, I., Rizzini, F., Piccin, A., 2017. The Alpine LGM in the boreal  
1245 ice-sheets game. *Sci. Rep.-UK*, 7, 2078. <https://doi.org/10.1038/s41598-017-02148-7>.  
1246  
1247 Moore, P.D., Webb, J.A., Collinson, M.E., 1991. *Pollen Analysis*. Blackwell Scientific Publications,  
1248 Oxford.  
1249  
1250 Mozzi, P., Bini, C., Zilocchi, L., Becattini, R., Mariotti Lippi, M., 2003. Stratigraphy, paleopedology  
1251 and palynology of Late Pleistocene and Holocene deposits in the landward sector of the lagoon of  
1252 Venice (Italy), in relation to the caranto level. *Il Quaternario* 16 (1Bis), 193-210.  
1253  
1254 Mozzi, P., 2005. Alluvial plain formation during the Late Quaternary between the southern Alpine  
1255 margin and the Lagoon of Venice (northern Italy). *Geogr. Fis. Din. Quat. (Suppl. 7)*, 219-230.  
1256  
1257 Mozzi, P., Piovan, S., Rossato, S., Cucato, M., Abbà, T., Fontana, A., 2010. Palaeohydrography and  
1258 early settlements in Padua (Italy). *Il Quaternario* 23, 387-400.  
1259

1260 Mozzi, P., Ferrarese, F., Fontana, A., 2013. Integrating digital elevation models and stratigraphic data  
1261 for the reconstruction of the post-LGM unconformity in the Brenta alluvial megafan (North-Eastern  
1262 Italy). *Alp. Mediterr. Quat.* 26, 41-54.

1263

1264 Müllenders, W., Favero, V., Coremans, M., Dirickx, M., 1996. Analyses polliniques de sondages à  
1265 Venise. In: Gullentops, F. (Ed.), *Pleistocene palynostratigraphy*. *Aardkundige Mededelingen* 7, 87-  
1266 117.

1267

1268 Müller, U.C., Pross, J., Bibus, E., 2003. Vegetation response to rapid climate change in Central  
1269 Europe during the past 140,000 yr based on evidence from the Fùramoos pollen record. *Quat. Res.*  
1270 59, 235-245.

1271

1272 Muttoni, G., Carcano, C., Garzanti, E., Ghielmi, M., Piccin, A., Pini, R., Rogledi, S., Sciunnach, D.,  
1273 2003. Onset of major Pleistocene glaciations in the Alps. *Geology* 31, 989-992.

1274

1275 Ninfo, A., Mozzi, P., Abbà, T., 2016. Integration of LiDAR and cropmarks remote sensing for the  
1276 study of fluvial and anthropogenic landforms in the Brenta-Bacchiglione alluvial plain (NE Italy).  
1277 *Geomorphology*. <http://dx.doi.org/10.1016/j.geomorph.2015.11.006>.

1278

1279 Okuda, M., Yasuda, Y., Setoguchi, T., 2001. Middle to Late Pleistocene vegetation history and  
1280 climatic changes at Lake Kopais, southeast Greece. *Boreas* 30, 73-82.

1281

1282 Pini, R., Ravazzi, C., Donegana, M., 2007. Gli ultimi cinque cicli climatici nella successione  
1283 sedimentaria della pianura friulana. In: Carli, B., Cavarretta, G., Colacino, M., Fuzzi, S. (Eds.), *Clima  
1284 e cambiamenti climatici: le attività di ricerca del CNR*, pp. 169-172.

1285

1286 Pini, R., Ravazzi, C., Donegana, M., 2009. Pollen stratigraphy, vegetation and climate history of the  
1287 last 215 ka in the Azzano Decimo core (plain of Friuli, north-eastern Italy). *Quat. Sci. Rev.* 28, 1268-  
1288 1290.

1289

1290 Pini, R., Ravazzi, C., Reimer P.J., 2010. The vegetation and climate history of the last glacial cycle  
1291 in a new pollen record from Lake Fimon (southern Alpine foreland, N-Italy). *Quat. Sci. Rev.* 29,  
1292 3115-3137.

1293

1294 Pola, M., Ricciato, A., Fantoni, R., Fabbri, P., Zampieri, D., 2014. Architecture of the western margin  
1295 of the North Adriatic foreland: the Schio-Vicenza fault system. *Italian J. Geosci.* 133, 223-234.

1296

1297 Reille, M., 1992e1995. *Pollen et spores d'Europe et d'Afrique du Nord*. Laboratoire de Botanique  
1298 historique et Palynologie, Marseille.

1299

1300 Reille, M., de Beaulieu, J.-L., 1995. Long Pleistocene pollen records from the Praclaux Crater, south-  
1301 central France. *Quaternary Res.* 44, 205-215.

1302

1303 Reille, M., Andrieu, V., de Beaulieu, J.-L., Guenet, P., Goeury, C., 1998. A long pollen record from  
1304 Lac du Bouchet, Massif Central, France for the period 325 to 100 ka (OIS 9c to OIS 5e). *Quat. Sci.*  
1305 *Rev.* 17, 1107-1123.

1306

1307 Rossato, S., Monegato, G., Mozzi, P., Cucato, M., Gaudio, B., Miola, A., 2013. Late Quaternary  
1308 glaciations and connections to the piedmont plain in the prealpine environment: the middle and lower  
1309 Astico Valley (NE Italy). *Quatern. Int.* 288, 8-24.

1310

1311 Rossato, S., Mozzi, P., 2016. Inferring LGM sedimentary and climatic changes in the southern  
1312 Eastern Alps foreland through the analysis of a <sup>14</sup>C ages database (Brenta megafan, Italy). *Quat. Sci.*  
1313 *Rev.* 148, 115-127.

1314

1315 Rossato, S., Carraro, A., Monegato, G., Mozzi, P., Tateo, F., 2018. Glacial dynamics in pre-Alpine  
1316 narrow valleys during the Last Glacial Maximum inferred by lowland fluvial records (northeast Italy).  
1317 *Earth Surf. Dynam.* 6, 809-828, 2018 <https://doi.org/10.5194/esurf-6-809-2018>.

1318

1319 Sánchez Goñi, M.F., Landais, A., Fletcher, W.J., Naughton, F., Desprat, S., Duprat, J., 2008.  
1320 Contrasting impacts of Dansgaard-Oeschger events over a western European latitudinal transect  
1321 modulated by orbital parameters. *Quat. Sci. Rev.* 27, 1136-1151.

1322

1323 Sidall, M., Stocker, T.F., Spahni, R., Blunier, T., McManus, J., Bard, E., 2006. Using a maximum  
1324 simplicity paleoclimate model to simulate millennial variability during the last four glacial cycles:  
1325 *Quat. Sci. Rev.* 25, 3185-3197.

1326

1327 Spötl, C., Holzkämper, S., Mangini, A., 2007. The last and the penultimate interglacial as recorded  
1328 by speleothems from a climatically sensitive high-elevation cave site in the Alps. In: Sirocko, F.,  
1329 Claussen, M., Sánchez Goñi, M.F., Litt, T. (Eds.), *The Climate of Past Interglacials. Development in*  
1330 *Quaternary Science*, vol. 7. Elsevier, pp. 471-491.

1331

1332 Spötl, C., Reimer, P.J., Starnberger, R., Reimer, R. 2013. A new radiocarbon chronology of  
1333 Baumkirchen, stratotype for the onset of the Upper Würmian in the Alps. *J. Quater. Sci.* 28, 552-558.

1334



1335 Stefani, C., Fellin, M.G., Zattin, M., Zuffa, G.G., Dalmonte, C., Mancin, N., Zanferrari, A., 2007.  
1336 Provenance and paleogeographic evolution in a multi-source foreland: the Cenozoic Venetian-  
1337 Friulian Basin (NE Italy). *J. Sediment. Res.* 77, 867-887. <https://doi.org/10.2110/jsr.2007.083>.  
1338  
1339 Stockmarr, J., 1971. Tablets with spores used in absolute pollen analysis. *Pollen et Spores* 13, 615-  
1340 621.  
1341  
1342 Toscani, G., Marchesini, A., Barbieri, C., Di Giulio, A., Fantoni, R., Mancin, N., Zanferrari, A., 2016.  
1343 The Friulian-Venetian Basin I: architecture and sediment flux into a shared foreland basin. *It. J.*  
1344 *Geosci.* 135. 1-54. 10.3301/IJG.2015.35.  
1345  
1346 Tzedakis, P.C., Andrieu, V., de Beaulieu, J.-L., Crowhurst, S., Follieri, M., Hooghiemstra, H., Magri,  
1347 D., Reille, M., Sadori, L., Shackleton, N.J., Wijmstra, T.A., 1997. Comparison of terrestrial and  
1348 marine records of changing climate of the last 500,000 years. *Earth Planet. Sci. Lett.* 150, 171-176.  
1349  
1350 Tzedakis, P.C., Andrieu, V., Beaulieu, J.-L. de, Birks, H.J.B., Crowhurst, S., Follieri, M.,  
1351 Hooghiemstra, H., Magri, D., Reille, M., Sadori, L., Shackleton, N.J., Wijmstra, T.A., 2001.  
1352 Establishing a terrestrial chronological framework as a basis for biostratigraphical comparisons. *Quat.*  
1353 *Sci. Rev.* 20, 1583-1592.  
1354  
1355 Tzedakis, P.C., McManus, J.F., Hooghiemstra, H., Oppo, D.W., Wijmstra, T.A., 2003. Comparison  
1356 of changes in vegetation in northeast Greece with records of climate variability on orbital and  
1357 suborbital frequencies over the last 450 000 years. *Earth Planet. Sci. Lett.* 212, 197-212.  
1358

1359 Tzedakis, P.C., Frogley, M.R., Lawson, I.T., Preece, R.C., Cacho, I., de Abreu, L., 2004. Ecological  
1360 thresholds and patterns of millennial scale climate variability: the response of vegetation in Greece  
1361 during the Last Glacial period. *Geology* 32 (2), 109-112.  
1362

1363 Udden, J.A., 1914. Mechanical composition of elastic sediments. *Bull. Geol. Soc. Am.* 25, 655-744.  
1364

1365 Van der Wiel, A.M., Wijstra, T.A., 1987. Palynology of the lower part (78-120 m) of the core Tenaghi  
1366 Philippon II. Middle Pleistocene of Macedonia. *Rev. Palaeobot. Palyno.* 52, 89-117.  
1367

1368 Venzo, S., 1977. I depositi quaternari e del neogene superiore nella bassa valle del Piave da Quero al  
1369 Montello e del Paleopiave nella valle del Soligo (Treviso), *Memorie Istituti Mineralogia Geologia*  
1370 *Università di Padova* 30, 1-64.  
1371

1372 Waelbroeck, C., Labeyrie, L., Michel, E., Duplessy, J.C., McManus, J.F., Lambeck, K., Balbon, E.,  
1373 Labracherie, M., 2002. Sea-level and deep water temperature changes derived from benthic  
1374 foraminifera isotopic records. *Quat. Sci. Rev.* 21, 295-305.  
1375

1376 Wagner, B., Vogel, H., Francke, A., Friedrich, T., Donders, T., Lacey, J.H., Leng, M., Regattieri, E.,  
1377 Sadori, L., Wilke, T., Zanchetta, G., Albrecht, C., Bertini, A., Combourieu-Nebout, N., Cvetkoska,  
1378 A., Giaccio, B., Grazhdani, A., Hauffe, T., Holtvoeth, J., Joannin, S., Jovanovska, E., Just, J., Kouli,  
1379 K., Kousis, I., Koutsodendris, A., Krastel, S., Lagos, M., Leicher, N., Levkov, Z., Lindhorst, K., Masi,  
1380 A., Melles, M., Mercuri, A.M., Nomade, S., Nowaczyk, N., Panagiotopoulos, K., Peyron, O., Reed,  
1381 J.M., Sagnotti, L., Sinopoli, G., Stelbrink, B., Sulpizio, R., Timmermann, A., Tofilovska, S., Totti,  
1382 P., Wagner-Cremer, F., Wonik, T., Zhang, X., 2019. Mediterranean winter rainfall in phase with  
1383 African monsoons during the past 1.36 million years. *Nature* 573, 256-260.  
1384 <https://doi.org/10.1038/s41586-019-1529-0>.

1385

1386 Wentworth, C.K., 1922. A scale of grade and class terms for clastic sediments. *J. Geology* 30, 377-  
1387 392.

1388

1389 Wohlfarth, B., Veres, D., Ampel, L., Lacourse, T., Blaauw, M., Preusser, F., Andrieu- Ponel, V.,  
1390 Kéravis, D., Lallier-Vergès, E., Björck, S., Davies, S.M., Beaulieu, J.-L., de Risberg, J., Hormes, A.,  
1391 Kasper, H.U., Possnert, G., Reille, M., Thouveny, N., Zander, A., 2008. Rapid ecosystem response  
1392 to abrupt climate changes during the last glacial period in western Europe, 40-16 ka. *Geology* 36 (5),  
1393 407-410.

1394

1395 Woillard, G., 1978. Grande Pile Peat Bog: A Continuous Pollen Record for the Last 140,000 Years.  
1396 *Quaternary Res.* 9(1), 1-21. doi: 10.1016/0033-5894(78)90079-0.

1397

1398 Zanferrari, A., Avigliano, R., Fontana, A., Paiero, G., (Eds) 2008. Note Illustrative della Carta  
1399 Geologica d'Italia alla scala 1:50.000: Foglio 087 "San Vito al Tagliamento". Graphic Linea,  
1400 Tavagnacco.

1401

1402

1403

1404

1405

1406

1407

1408

1409

1410

1411 **Figure captions**

1412 **Fig. 1**

1413 Location of the Geriatrico 1 (GER1) and Cà Borille (CB) cores and the reference records of the  
1414 Venetian-Friulian plain discussed in the text (base map modified from Fontana et al., 2008).

1415

1416 **Fig. 2**

1417 Stratigraphic logs of Geriatrico 1 (GER1) and Cà Borille (CB) cores. Calibrated  $^{14}\text{C}$  ages, identified  
1418 stratigraphic units as well all the treated pollen and micropaleontological samples are reported. The  
1419 dashed line indicated the main stratigraphic correlation discussed in the text.

1420

1421 **Fig. 3**

1422 Overview pollen diagram of Geriatrico 1 (GER1) core with selected % records. *Alnus*, Poaceae,  
1423 Cichorioideae, hydrophytes and hygrophytes are excluded from the Upland Pollen Sum. Only pollen  
1424 samples with Upland Pollen Sum greater than 100 grains are reported. Black dots indicate percentage  
1425 values < 1%.

1426 Hydrophytes include *Hydrocaris*, *Menyanthes trifoliata*, *Myriophyllum spicatum* type, *Myriophyllum*  
1427 *verticillatum* type, *Nuphar*, *Nymphaea alba* and *Potamogeton natans*.

1428 Hygrophytes include Cyperaceae, *Lythrum salicaria* type, *Sparganium* type and *Typha latifolia* type.

1429

1430 **Fig. 4**

1431 Overview pollen diagram of Cà Borille (CB) core with selected % records. *Alnus*, Poaceae,  
1432 Cichorioideae, hydrophytes and hygrophytes are excluded from the Upland Pollen Sum. Only pollen  
1433 samples with Upland Pollen Sum greater than 100 grains are reported. Black dots indicate percentage  
1434 values < 1%.

1435 Hydrophytes include *Callitriche*, *Menyanthes trifoliata*, *Myriophyllum alterniflorum* type,  
1436 *Myriophyllum spicatum* type, *Myriophyllum verticillatum* type, *Nuphar*, *Nymphaea alba*,  
1437 *Potamogeton* subg. *P.* type, *Stratiotes aloides* and *Trapa natans*.

1438 Hygrophytes include *Alisma plantago aquatica*, Cyperaceae, *Filipendula* cf. *ulmaria*, *Hottonia*  
1439 *palustris*, *Lythrum salicaria* type, *Sparganium* type, *Thalictrum* and *Typha latifolia* type.

1440

1441 **Fig. 5**

1442 Stratigraphic and chronological correlation between Geriatrico 1 (GER1) and Cà Borille (CB) cores,  
1443 based on the multi-proxy information. Specific percentage pollen histograms are selected and  
1444 integrated with stratigraphic and micropaleontological data.

1445 *Pinus*: cumulative percentage of *Pinus cembra*, *Pinus diploxylon* and *Pinus haploxylon*.

1446 Broad-leaved trees and shrubs: cumulative percentage of *Carpinus* type, *Buxus*, *Cornus mas* type,  
1447 *Cornus sanguinea* type, *Corylus*, *Fagus sylvatica* type, *Frangula alnus*, *Fraxinus*, *Olea europea*,  
1448 *Quercus robur* group, *Tilia*, *Ulmus*, *Ulmus-Zelkova*, *Vitis vinifera* and *Zelkova*.

1449 Xerophytes: cumulative percentage of *Artemisia*, Chenopodiaceae, *Ephedra distachya* type, *Ephedra*  
1450 *fragilis* type, *Hippophae rhamnoides*.

1451

1452 **Fig. 6**

1453 Correlation between playnological and stratigraphic data of Geriatrico 1 (GER1) and Cà Borille (CB)  
1454 cores and the global marine records over the last 220 ka. The selected percentage pollen records of  
1455 Fig. 5 are plotted against a temporal y axis and compared with the marine  $\delta^{18}\text{O}$  LR04 stack curve by  
1456 Lisiecki and Raymo (2005). The marine-transitional intervals are correlated with the curve of global  
1457 sea-level oscillations by Waelbroeck et al. (2002).

1458

1459

1460

1461 **Table captions**

1462 **Tab. 1**

1463 Radiocarbon dates obtained for GER1 and CB cores. AMS: Accelerator Mass Spectrometry (ETH  
1464 Zürich for GER1 and Tandem Laboratory, University of Uppsala for CB core). <sup>14</sup>C ages are  
1465 calibrated with the online calibration programme OxCal (version 4.3, calibration curve IntCal13;  
1466 Bronk Ramsey, 2009).

1467

1468 **Tab. 2**

1469 The main features of paleosoils within the GER1 and CB stratigraphic successions. Estimate of the  
1470 degree of soil development: \* poorly developed; \*\* moderately developed; \*\*\* well developed.

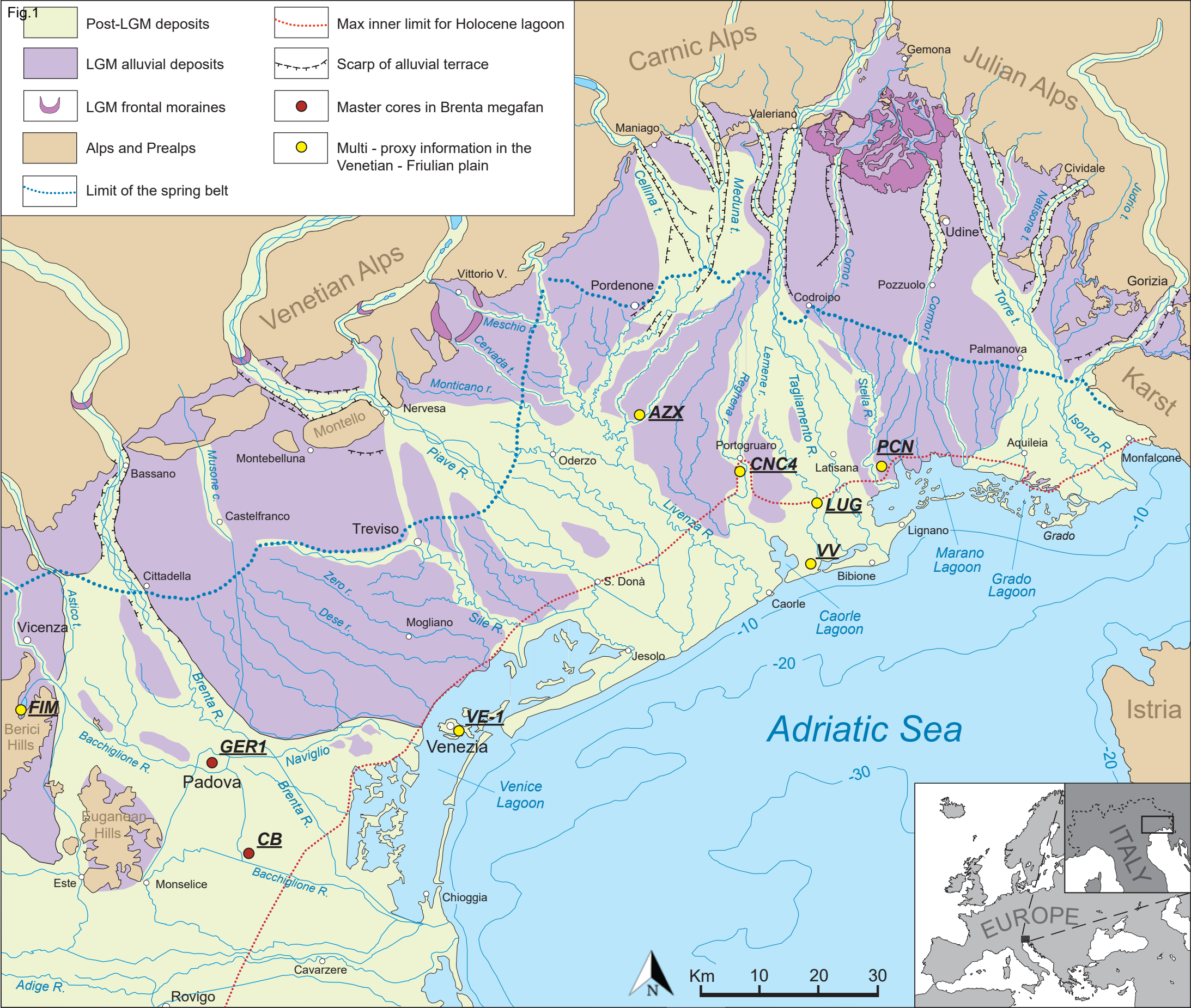
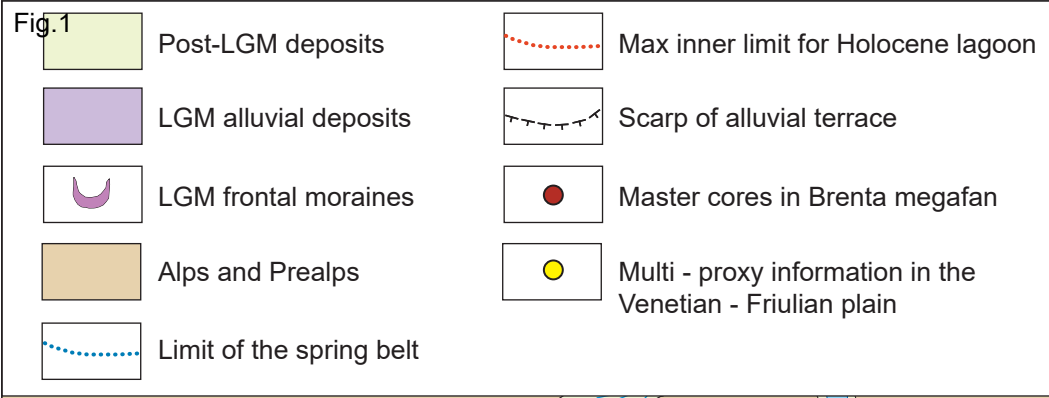


Fig.2

GER1 core

CB core

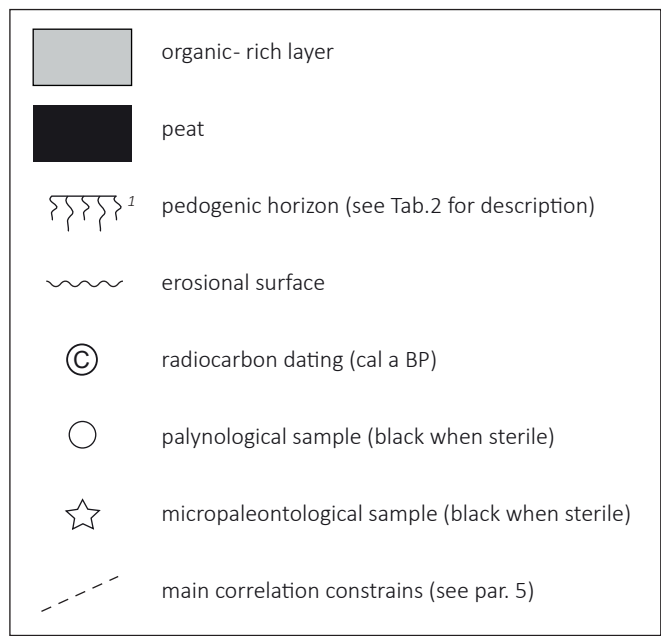
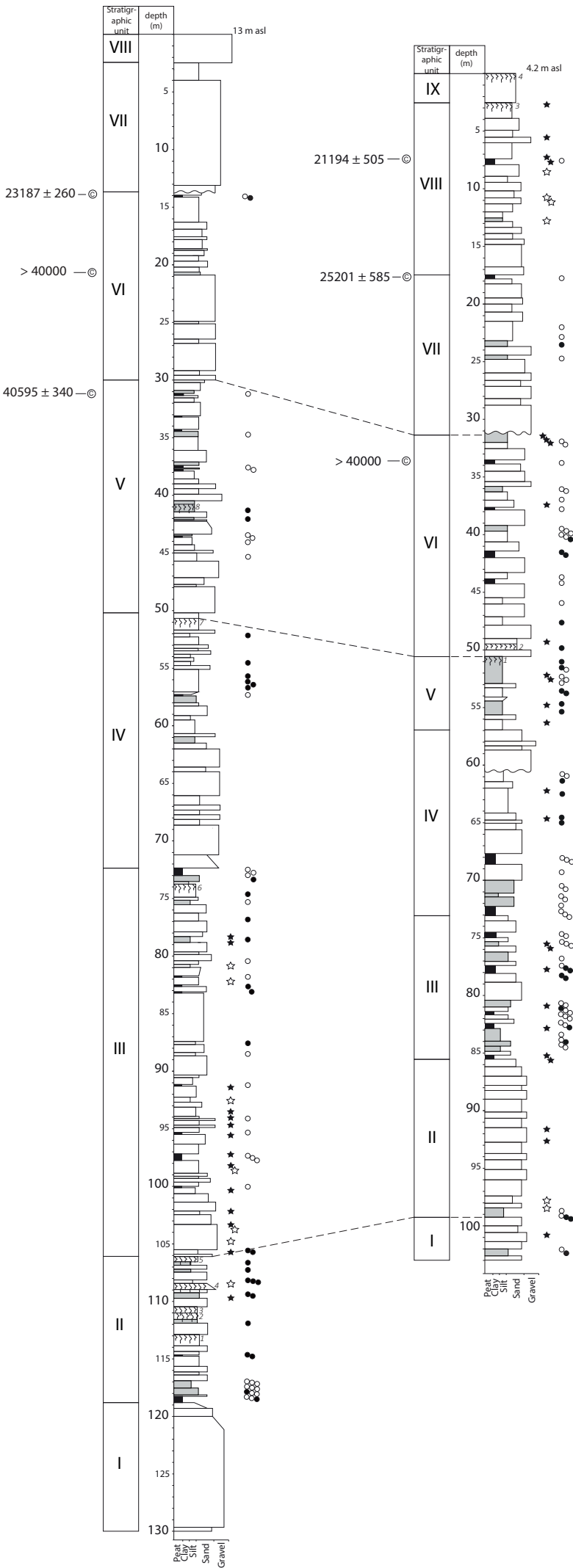




Fig.3

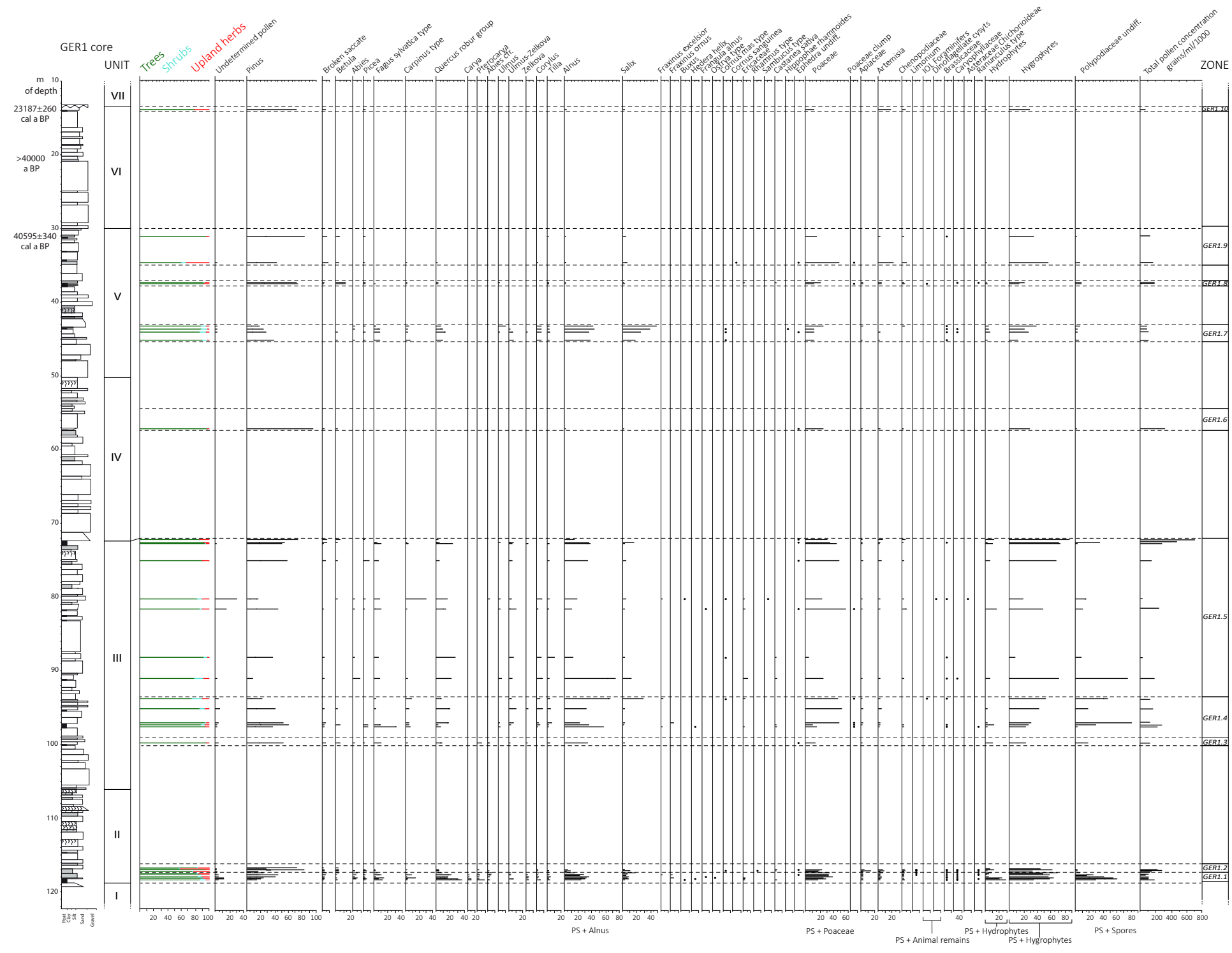
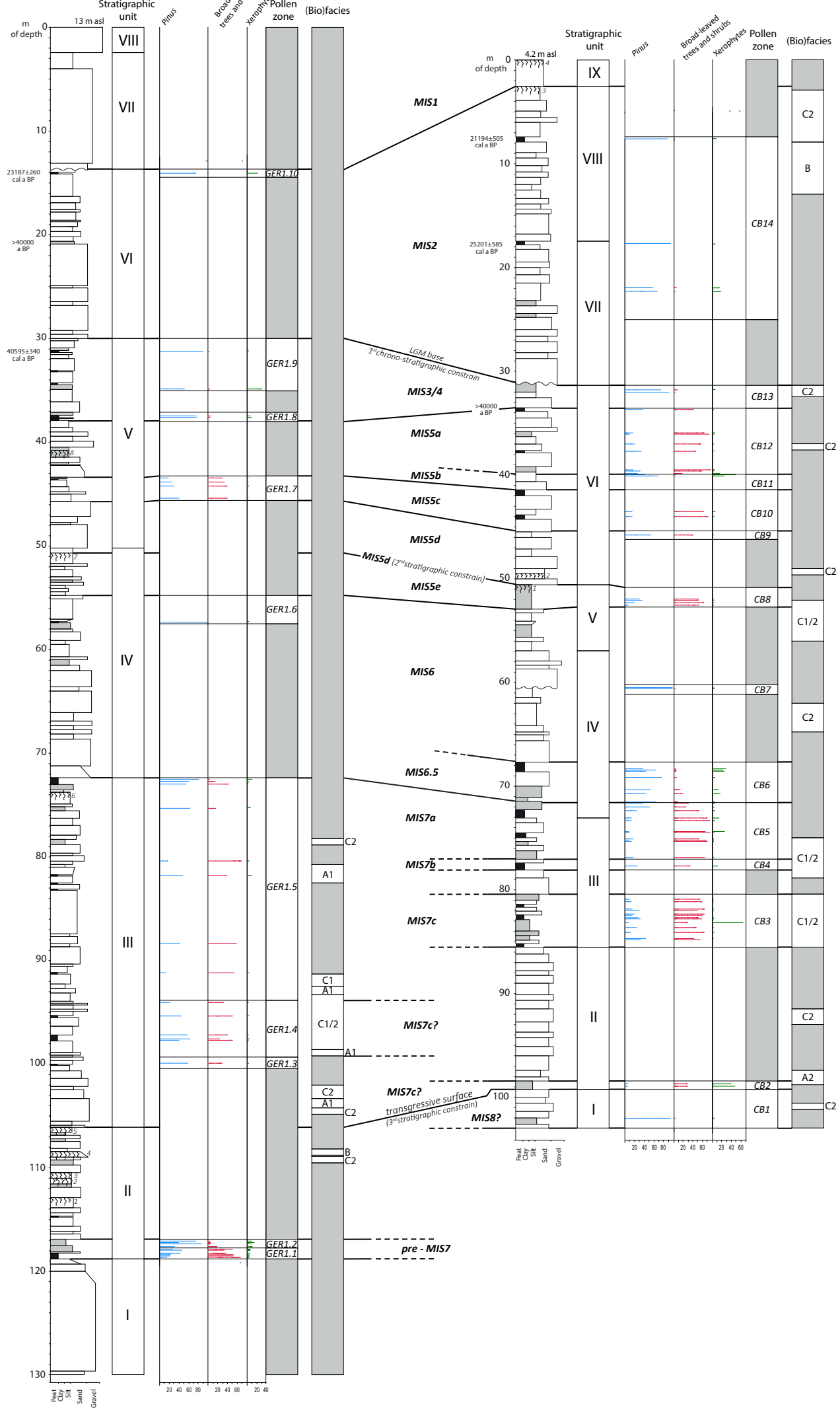




Fig.5

# GER1 core

# CB core







[Click here to access/download](#)

**Table**

Tab. 1.docx





Click here to access/download

**Table**

Tab. 2.docx



**Declaration of interests**

The authors declare that they have no known competing financial interests or personal relationships that could have appeared to influence the work reported in this paper.

The authors declare the following financial interests/personal relationships which may be considered as potential competing interests:

## **Author Statement**

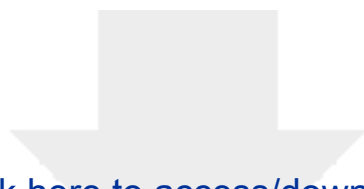
All authors contributed substantially to the research. Arianna Marcolla: Investigation, Data analysis, Writing – Original draft preparation; Antonella Miola: Investigation, Methodology, Data analysis; Paolo Mozzi: Conceptualization, Investigation, Writing – Review & Editing; Giovanni Monegato: Conceptualization, Validation, Writing – Review & Editing; Alessandra Asioli: Investigation, Data analysis; Roberta Pini: Validation; Cristina Stefani: Conceptualization, Supervision.





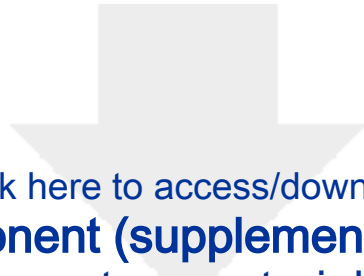
Click here to access/download  
**e-Component (supplementary data)**  
Supplementary material 1.tgx





Click here to access/download  
**e-Component (supplementary data)**  
Supplementary material 2.tgx





Click here to access/download  
**e-Component (supplementary data)**  
Supplementary material 3.docx





Click here to access/download  
**e-Component (supplementary data)**  
Supplementary material 4.docx

